

**High Pressure Vibrational Spectroscopic Studies of
Some Organoplatinum Complexes**

by

Jean A. Baldwin

*A thesis submitted to the Faculty of Graduate Studies and
Research of McGill University in partial fulfillment of the
requirements for the degree of Master in Science.*

July 1992

Department of Chemistry

McGill University

Montreal, Quebec, Canada

© Jean A. Baldwin

**Vibrational Spectroscopic Studies of
Some Organoplatinum Complexes**

*To my parents, Margaret and Eugene Baldwin
for their love and support throughout my education*

ABSTRACT

High pressure infrared and micro-Raman vibrational spectroscopy has been used to study the following organoplatinium(II) complexes: Zeise's salt, $K[Pt(\eta^2-C_2H_4)Cl_3]$; Zeise's dimer, $[Pt(\eta^2-C_2H_4)_2Cl_2]_2$; and dichloro(1,5-cyclooctadiene)platinum(II), $Pt(COD)Cl_2$. Pressure dependences of the vibrational modes have been used in the assignments of the $\nu(C=C)$ modes and the ethylene and cyclic diene C-H stretching vibrations. Pressure increases the extent of π -backbonding, as shown by the negative pressure dependence of the $\nu(C=C)$ stretching frequencies.

RÉSUMÉ

La spectroscopie vibrationnelle infrarouge à haute pression et micro-Raman à haute pression ont été utilisées pour étudier les complexes organoplatinum (II) suivants: le sel de Zeise, $K[Pt(\eta^2-C_2H_4)Cl_3]$; le dimer de Zeise, $[Pt(\eta^2-C_2H_4)_2Cl_2]_2$; et dichloro(1,5-cyclooctadiène)platine(II), $Pt(COD)Cl_2$. La dépendance des modes vibrationnels sur la pression a été utilisée pour la classification des modes $\nu(C=C)$ et les vibrations d'étirement C-H du diène cyclique. La pression augmente le degré de π -retrodonation, ceci est démontré par la dépendance négative de la fréquence d'étirements $\nu(C=C)$ sur la pression.

ACKNOWLEDGMENTS

I would like to express my sincere gratitude to Professors Ian Butler and Denis Gilson for their guidance and encouragement throughout the course of this work and most especially during the writing of this thesis.

I would also like to thank:

my colleagues Mr. Y Huang, and Mrs. H.Qi Li for introducing me to the techniques of high pressure vibrational spectroscopy;

Dr. Ross Markwell and Steve Barnett for their assistance on the IR and Raman spectrometers;

Mr. R. Rossi for his technical expertise;

Dr. J. Mo for his criticisms and suggestions throughout this work.

Dave Pinto for translating the abstract into French.

Mark Wall for his assistance in the writing of this thesis;

and all of my friends in the Otto Mass Chemistry department for their encouragement and support throughout the course of this work.

Financial support from the Department of Chemistry, McGill University in the form of a teaching assistantship is gratefully acknowledged.

NOTE ON UNITS

The guidelines concerning Thesis Preparation from the Faculty of Graduate Studies and Research specify that the use of SI units is mandatory.

The following units have been used in this thesis for historical reasons. Their definitions and SI equivalents are given below:

Physical quantity	symbol	SI unit	unit used
wavenumber	ν	m^{-1}	cm^{-1} (=100 m^{-1})
pressure	p	Pa (Nm^{-2})	kbar (=108 Pa)
force constant	k	Nm^{-1}	dyne cm^{-1} (=103 Nm^{-1})
bond length	r	m	Å (=10 ⁻¹⁰ m)

In the text of this thesis, the unit of vibrational wavenumber is often referred to as the vibrational frequency (ν). These quantities are directly proportional to one another, $\nu = c\bar{\nu}$, where c is the speed of light.

LIST OF ABBREVIATIONS

The following abbreviations have been used in this thesis.

COD	1,5-cyclooctadiene
C ₂ H ₄	η^2 -C ₂ H ₄
DAC	diamond anvil cell
CO	carbonyl
IR	infrared
NBD	norbornadiene
NMR	nuclear magnetic resonance
NQR	nuclear quadrupole resonance
CN	cyano

TABLE OF CONTENTS

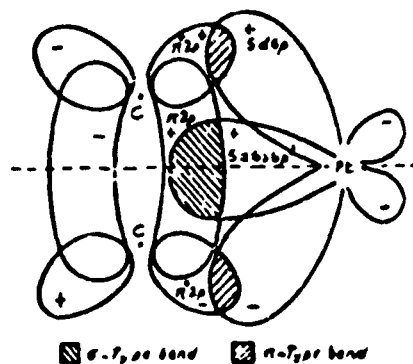
	page
Abstract.....	iii
Resume.....	iv
Acknowledgments.....	v
List of Abbreviations.....	vi
Note on Units.....	vii
CHAPTER 1. INTRODUCTION.....	1
CHAPTER 2 VIBRATIONAL SPECTROSCOPY - A GENERAL	
INTRODUCTION	12
2.2 Infrared Absorption.....	13
2.3 Raman Scattering	13
2.4 Normal Modes of Vibration	15
2.6 Factor Group Analysis - Zeise's Salt.....	18
2.7 Pressure Effects on Crystals.....	19
CHAPTER 3. EXPERIMENTAL	23
3.1 High-pressure Infrared Spectra	23
3.2 High-pressure Micro-Raman Spectra.....	24
3.3 Sample Source and Purity	25
CHAPTER 4. SPECTROSCOPIC STUDIES ON ZEISE'S SALT	
K[Pt(η^2-C₂H₄)Cl₃].....	27
4.1. Vibrational Assignments.....	27
4.2 Solid State Symmetry.....	30
4.3 High Pressure Effects.....	31
CHAPTER 5. ZEISE'S DIMER [Pt(η^2-C₂H₄)Cl₂]₂	45
5.1 Introduction.....	45
5.2 High Pressure Effects.....	48

CHAPTER 6. Dichloro (1,5-cyclooctadiene)platinum (II): Pt(COD)Cl₂	56
6.1 Introduction	56
6.2 Factor group analysis	56
6.3 High Pressure Effects.....	57
CHAPTER 7. CONCLUSIONS.....	73

CHAPTER 1
INTRODUCTION

Olefin complexes are the oldest class of organometallic compounds known. The first example $\text{Pt}(\eta^2\text{-C}_2\text{H}_4)\text{Cl}_3\cdot\text{H}_2\text{O}$, known as Zeise's salt,¹ was reported in 1830. Olefin complexes of platinum have been extensively studied because of their greater kinetic stability than their palladium analogues, which, because of their lower stability, are catalytically more useful. Zeise's salt has become one of the most cited examples of the Dewar-Chat-Duncanson (D-C-D)^{2,3} model of metal-olefin complexation. This molecular orbital formalism essentially involves a σ bond (olefin-to-metal) and π bond (metal-to-olefin), as shown in Figure 1.1.1.

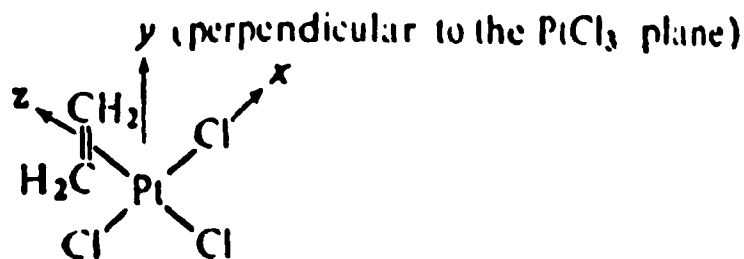
Figure 1.1.1. (from ref. 3)



The σ bond is formed by donation of charge from the π -orbital on the olefin to the empty $5d6s6p^2$ hybrid orbital on platinum and the π bond is formed by the backdonation of charge from the filled $5d6p$ hybrid orbital on platinum to the empty π^* -orbital on the olefin. X-ray crystallographic studies have established that alkenes coordinated to the d^8 transition metals display definite conformational preferences in the solid state. In the square-planar d^8 complexes, the alkene carbon is perpendicular to the square plane defined by, in the case of Zeise's salt, the PtCl_3 moiety. For the x, y, z axes

shown in Figure 1.1.2, the backdonation from the $5d_{yz}6p_y$ hybrid orbital on the platinum to the π^* -orbital on ethylene requires a perpendicular ethylene orientation.

Figure 1.1.2

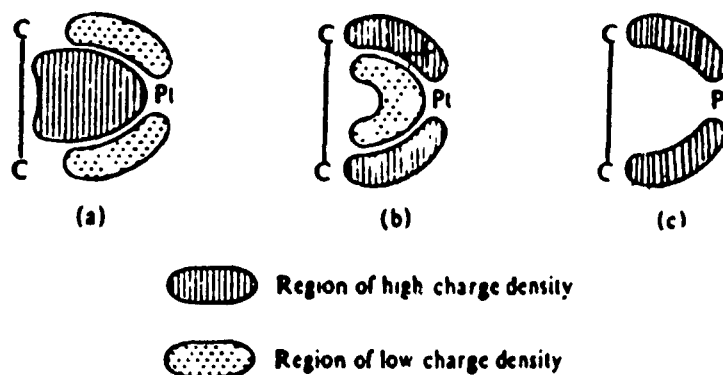


Rotational barriers about the metal-olefin bond axis, measured by solution NMR spectroscopy,⁴ show a small activation energy of between 10-25 kcal mol⁻¹ and reflect the fact that the preferred ground-state conformation with a perpendicular ethylene arises from a combination of steric and electronic effects.^{4,5,15,19} The electronic component is easy to appreciate in terms of the D-C-D model. The totally symmetric σ orbital is insensitive to the ethylene orientation; in contrast, the alkene π^* orbital can overlap with either the d_{yz} or the d_{xz} metal orbital. Thus, the electronic component of the rotational barrier will be sensitive to the relative energies of the metal d_{xz} and d_{yz} orbitals in the ML_3 fragment. For an ML_3 molecule with C_{2v} symmetry, the d_{xz} and d_{yz} orbitals of the ethylene are non-degenerate.⁵ If their energies differ significantly, then the rotational barrier is mostly electronic in origin. Extended Huckel calculations⁶ for the PtCl₃ moiety gave an energy difference of 0.4 eV between the d_{yz} and d_{xz} orbitals. Since the $d_{yz}p_y$ hybrid orbital involves an unoccupied π -orbital, it can strengthen the metal-olefin bond by increasing the overlap capability of the metal $d\pi$ -orbital. It is predicted that the $5d_{xz}$ orbital will give less overlap, because the p_x orbital is involved in bonding to the cis-chlorine ligands.¹⁵ The lower energy d_{yz} orbital leads to only a slight preference for the

perpendicular conformation. This lower energy accounts for the metal-olefin rotation. Consequently, the steric effects, which arise from the close proximity of the cis chlorines and the alkenic carbons in the in-plane conformation, constitute the main component in achieving the ethylene out-plane conformation.¹⁹ It has been estimated that approximately 70% of the observed conformation barrier arises from the steric effects and only 30% from the electronic effects.⁷ Subsequent MO calculations⁸ gave the total energy of the Pt-olefin complex as a function of the angle between C=C double bond axis and the PtCl₃ plane. The energy minima observed when the olefin lies at 0° and 90° to the Pt square plane are similar in depth, so the perpendicular arrangement is also related to the steric interactions. The D-C-D synergic bonding model has a flexibility which has proved invaluable in rationalising the physical and chemical properties of Zeise's salt and a range of alkene complexes. The following observations have been discussed in terms of the σ and π bonding: (1) The weakening and lengthening of the C=C double bond, detected by X-ray and IR studies, are the result of both the loss of electron density in the olefin π -orbital and the gain of electron density in the olefin π^* -orbital. Ab initio calculations on Zeise's salt revealed the equilibrium C=C bond length in terms of the total energy to be longer than that of the free ethylene by 0.053 Å (0.038 Å experimentally). (2) The high trans effect of olefins, as defined by kinetic studies, is a result of the withdrawal of charge from the metal to the olefin π^* -orbital stabilising a 5-coordinated trigonal-bipyramidal state. There is no clear evidence to show the bond weakening trans influence of trans σ -bonded ligands (or weak π -bonded ligands, e.g., Pt-Cl),⁹ since only ligands which exert their trans effect by a π -acceptor mechanism will cause weakening if the trans bond has a π -component. (3) The ¹H NMR spectra of Pt-olefin complexes show a decrease in both the cis and trans proton-proton coupling constants on coordination of the olefin as the initial sp² hybrid of the C atoms is altered towards a sp³ hybrid.¹⁰ (4) The groups bound to the olefin carbon atoms are bent out of the plane of the double bond away from the platinum. The electronic density is shifted towards the C-R bonds due to

the π -backbonding, where the R substituents on the olefinic carbons are R = H, halogens, and bulky groups. This will repel the C-R bonds by bond pair/bond pair repulsion and so force R away from the metal.¹¹ The bending back is least for hydrogen and greatest for the halogen substituents. This parallels the metal-alkene bond lengths where the shortest distances are associated with the halogen substituted alkenes.⁸ From a CNDO MO study, cis-bending of substituents is favoured.¹² In Zeise's salt, the hydrogen atoms are bent back $\sim 32.5^\circ$ from the normals to the CH_2 plane.¹³ In complexes bearing strong electronegative substituents on the alkene and containing a metal of low oxidation state, the bonding goes beyond that of the D-C-D model and approaches that of a metallopropane structure represented in valence bond terms as two σ carbanion bonds.^{14,15} Figure 1.1.3 depicts the effect of the distribution of electron density in the region between the metal and olefin when the relative importance of the σ and π components of the metal-olefin bond are altered.

Figure 1.1.3



The carbon hybridisation scheme (b) between the two extremes (a) sp^2 and (c) sp^3 carbon bonds best describes the synergistic bonding in Zeise's salt.¹⁵ Although the features of this model are now accepted, there remains some controversy over the relative extent of the σ and π contributions in stabilising the Pt-ethylene interaction.

X-ray Diffraction Studies

X-ray investigations of Zeise's salt have been inconsistent, as strong scattering from the platinum atom has made refinement of the positions of the lighter atoms difficult.¹⁶ A more accurate study by neutron diffraction¹³ gave a C=C bond distance of 1.375 Å, i.e., 0.038 Å longer than free ethylene and shorter than previously reported. The olefin double bond forms an angle of 5.9° with the normal to the PtCl₃ plane. These details imply a weaker π -backbonding contribution.

NMR Studies

This technique was used to provide preliminary evidence for the structure of metal-olefin complexes and also afforded valuable information on the rotation of the olefin group and possible changes in the hybridisation. Earlier proton NMR spectra on single crystals of Zeise's salt and its deuterium oxide analogues were recorded at a number of orientations relative to the magnetic field and suggested that the ethylene molecule was undergoing large amplitude rotational oscillations about both the Pt-olefin bond and the C=C double bond axis.¹⁷ This implies a significantly weak π backbonding. In contrast, the results of a ¹H NMR¹⁸ study on polycrystalline [Pt(η^2 -C₂H₄)Cl₂]₂ did not show any evidence for the rotation about the Pt-olefin bond, instead a rocking motion about this axis and a twist about the C=C axis were suggested. The olefin bond lengthening and the bent C-H plane are consistent with the results from the monomer X-ray diffraction. Variable-temperature ¹H NMR showed that two resonance signals coalesce on warming, which was interpreted as a rapid Pt-olefin rotation (on the NMR timescale). Other interpretations have been suggested, including a rapid intermolecular exchange,²³ but none was consistent with all the experimental data. From the coalescence temperature, the energy barriers³ for d⁸ Pt-olefin complexes are estimated to

be relatively low, between 10-15 kcal mol⁻¹. Ab initio studies¹⁹ have given, for Zeise's salt, a value of 15 kcal mol⁻¹. However, from solution NMR measurements there is an upfield proton chemical shift²¹ on coordination to the Pt(II); in Zeise's salt, the shift τ is from 4.63 to 5.17 ppm. More electronegative substituents on the olefin cause the chemical shift to move increasingly upfield.²¹ There is also a similar upfield chemical shift in the ¹³C resonances²² of coordinated olefin carbons from 123 ppm for the free ethylene to 63 and 77 ppm for Zeise's salt and the dimer, respectively. The larger chemical shift values indicate greater electron density on the olefinic protons from the π -backbonding with the resultant increase in magnetic shielding. Both cis and trans coupling constants of the olefin decrease on coordination to Pt, implying sp³ hybridisation.²⁰ Contrary to the earlier studies, the most recent ¹³C NMR work²² on Zeise's salt and the dimer showed no rotation about the metal-olefin axis as the chemical shift tensor was not averaged by the motion. The ¹H and ¹³C NMR chemical shifts correlate linearly with the percentage lowering of the C=C stretching modes in the IR spectrum, and inversely with the C=C bond lengthening.²⁴

Vibrational Spectroscopic Studies

The IR and Raman spectra of Pt(II)-olefin complexes have been studied extensively and the research has been focused primarily on the metal-olefin interaction.²⁵ An accurate knowledge of the frequencies can give a considerable amount of information on the structure and bonding in the molecule. However, the vibrational assignments have proved to be very difficult for a number of reasons. The symmetry of the compounds tends to be very low, Zeise's salt has C_{2v} symmetry, and so many of the fundamental modes have the same symmetry and are coupled. The assigned symmetric C=C stretching mode is very weak in the IR and since it is coupled to other modes, there is no direct relation between the frequency shift upon coordination and the strength of the Pt-

direct relation between the frequency shift upon coordination and the strength of the Pt-olefin bond.²⁶ There have been numerous vibrational studies of Zeise's salt and the dimer reported in the literature, but there still remains some controversy over the correct assignments. Being the simplest of the metal-olefin compounds available, it is advantageous that the vibrational spectrum is assigned confidently. This topic is discussed further in Chapter 4.

ESCA Studies

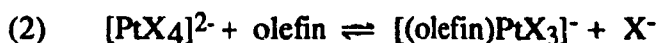
It is evident that the electron density on the olefin and the resultant changes in bond length, nuclear shielding and vibrational modes are related to the lower ionization potential of the metal atoms on coordination. It is not clear whether this effect is caused by the inhibition of the forward σ -donation or by the enhancement of the π -backbonding. Electron spectroscopy for chemical analysis (ESCA) was applied as a means of probing the electron density on the metal. The binding energy of the metal electrons increased slightly from 73.9 to 74.5 eV on replacing a chlorine in $[\text{PtCl}_4]^{2-}$ by an olefin, indicative of some π -backbonding.²⁷

³⁵Cl NQR Studies

The ³⁵Cl NQR frequencies of Zeise's salt²⁸ and Pt(COD)Cl₂ are 20.13 (cis-Cl) and 19.77 MHz, respectively. These are shifted upfield from K₂[PtCl₄] at 17.93 MHz. The increased ³⁵Cl frequency was attributed to stronger π -backbonding which increased the σ covalency of the Pt-Cl bond.

Stability Studies

The affinities of simple olefins for Pt(II) have been compared in two systems by measuring by spectrophotometrical methods the equilibrium constants²⁹⁻³¹ for olefin displacement:



Since the structure of the olefin was modified so as to decrease the electron density at the olefin bond, the equilibrium constant decreased. For example, as the extent of alkyl substitution on the olefin was increased, the equilibrium constant decreased (from ~ 5 to ~ 7) and the enthalpy of reaction ΔH , became more negative. It was concluded that that the π -acceptor bond was more important than than the σ bond in increasing the stability of the metal-olefin bond.

A successful attempt was made to correlate the change in $\nu(\text{C}=\text{C})$ on coordination with the change in electron density on the Pt(II) ion.³² A series of pyridine N-oxide (Q) derivatives of the type $\text{trans-Pt}(\text{C}_2\text{H}_4)(\text{Q})\text{Cl}_2$, showed a $\nu(\text{C}=\text{C})$ decrease with increasing electronegativity of Q. There was a linear pK_a correlation with $\nu(\text{C}=\text{C})$, as well as with the Taft σ values with the substituent Q. It was concluded that the greater the electron donation power of the substituents, the stronger the Pt-olefin π -backbonding became.

Theoretical Studies

The nature of the metal-olefin bond has been the subject of numerous theoretical studies. The calculated relative extent of the π -backbonding in Zeise's salt is as varied as are the experimental conclusions. From SCF MO calculations,³³ it was shown that the

C=C force constant of approximately $6.55 \text{ mydn } \text{\AA}^{-1}$ gave a bond order close to 1.6. On the other hand, an ab initio MO study³⁴ suggested the σ donation to be the more dominant factor in bonding, but a later analysis of orbital population¹⁹ showed a near equal electron transfer for both the σ and π bonds.

Thesis Objective

High-pressure vibrational spectroscopy has generally been used to show order-disorder phase changes under external pressures in a wide range of compounds, including organic plastic crystals³⁵ and high symmetry inorganic complexes.^{36,37} More recently, the pressure sensitivities of organometallic complexes and, in particular, metal carbonyl compounds,³⁸ have been investigated.

In this thesis, high-pressure IR and Raman spectroscopy are used to show the presence of π backbonding in three Pt-olefin compounds. The pressure dependences of the vibrational modes were measured, and the behaviour of the frequency shifts with pressure allow a more confident assignment of the $\nu(\text{C}=\text{C})$ stretching modes and the assessment of the extent of π backbonding which occurs with pressure. The pressure dependence of the $\nu(\text{Pt-olefin})$ stretching modes were also measured and the compressibility of the metal-olefin bond is evaluated in terms of the increased π -backbonding to the C=C bonds.

REFERENCES

- (1) Zeise, W. C. *Mag. Pharm.* **1830**, 35, 45-54.
- (2) Dewar, M. J. S. *Bull. Soc. Chem. Fr.* **1951**, 18, 79.
- (3) Chatt, J.; Duncanson, L. A. *J. Chem. Soc.* **1953**, 2939.
- (4) Holloway, C. E.; Hulley, G.; Johnson, B. F. G.; Lewis, J. *J. Chem. Soc. (A)* **1969**, 53.
- (5) Mingos, D. M. P. *Comprehensive Organometallic Chemistry*; Pergamon: New York, 1982; Vol. 3, Ch. 19.
- (6) Albright, T. A.; Hoffman, R.; Thibeault, J. C.; Thorn, D. Q. *J. Am. Chem. Soc.* **1979**, 101, 3801.
- (7) Baddley, W. H., *J. Am. Chem. Soc.* **1968**, 90, 3705.
- (8) Zeigler, T.; Rauk, A. *Inorg. Chem.* **1979**, 18, 1558.
- (9) Green, M.; Osbourne, R. B. L.; Rest, A. J.; Stone, F. G. *Chem. Commun.* **1966**, 502.
- (10) Chatt, J.; Duncanson, L. A.; Venanzi, L. M. *J. Chem. Soc.* **1955**, 4456.
- (11) Gillespie, R. J.; Nyholm, R. S. *Quart. Rev.* **1957**, 11, 339.
- (12) Blizzard, A. C.; Santry, D. P. *J. Chem. Soc.* **1968**, 90, 5749.
- (13) Love, R. A.; Koerzie, T. F.; Williams, G. F.; Andrews, L. A.; Bau, R. *Inorg. Chem.* **1975**, 14, 2653.
- (14) Panattoni, C.; Bombieri, G.; Belluco, U.; Buddley, W. H. *J. Am. Chem. Soc.* **1968**, 90, 798.
- (15) Hartley, F. R. *Comp. Organ. Met. Chem.* **1982**, vol. 6.
- (16) Black, M.; Mais, R. H. B.; Owston, P. G. *Acta Cryst.* **1969**, B25, 1753.
- (17) Maricic, S.; Redpath, C. R.; Smith, J. A. *J. Chem. Soc.* **1963**, 4905.
- (18) Reeves, L. W. *Can. J. Chem.* **1960**, 38, 736.
- (19) Hay, P. J. *J. Am. Chem. Soc.* **1981**, 103, 1390.

- (20) (a) Holloway, C. E.; Hulley, G.; Johnson, B. F. G.; Lewis, J. J. *Chem. Soc. (A)* **1970**, 1653.
(b) Holloway, C. E.; Hulley, G.; Johnson, B. F. G.; Lewis, J. J. *Chem. Soc. (A)* **1969**, 53.
- (21) Kistner, C. R.; Doyle, J. H.; Storlie, J. C. *Inorg. Chem.* **1963**, 2, 1255.
- (22) Huang, Y.; Ph.D. Thesis, McGill University, Montreal, 1992.
- (23) Kaplan, P. D.; Schmidt, P.; Orchin, M. *J. Am. Chem. Soc.* **1967**, 89, 4537.
- (24) Ittel, S. D.; Ibers, J. A. *Adv. Organomet. Chem.* **1976**, 14, 33.
- (25) Davidson, G. *Organometal. Chem. Rev. A* **1972**, 8, 303.
- (26) Hartley, F. R. *Chem. Rev.* **1969**, 799.
- (27) Clark, D. T.; Briggs, D.; Adams, D. B. *J. Chem. Soc., Dalton Trans.* **1973**, 169.
- (28) Yesinowski, J. P.; Brown, T. L. *Inorg. Chem.* **1971**, 10, 1097.
- (29) Joy, J. R.; Orchin, M. *J. Am. Chem. Soc.* **1959**, 81, 310.
- (30) Denning, R. G.; Hartley, F. R.; Venanzi, L. M. *J. Chem. Soc. (A)* **1967**, 324.
- (31) Denning, R. G.; Hartley, F. R.; Venanzi, L. M. *J. Chem. Soc. (A)* **1967**, 328.
- (32) Shupack, S. I.; Orchin, M. *J. Am. Chem. Soc.* **1963**, 85, 902.
- (33) Kâto, H. *Bull. Chem. Soc. Jpn.* **1971**, 44, 348.
- (34) Andrews, D. C.; Davidson, G.; Duce, D. A. *J. Organomet. Chem.* **1975**, 1014, 113.
- (35) Haines, J.; Ph.D. Thesis, McGill University, Montreal, 1989.
- (36) Huang, Y.; Butler, I. S. *J. Raman Spectrosc.* **1990**, 21, 273.
- (37) Paroli, R. M.; Kawai, N. T.; Lord, G.; Butler, I. S.; Gilson, D. F. R. *Inorg. Chem.* **1989**, 28, 1819.
- (38) Huang, Y.; Butler, I. S.; Gilson, D. F. *Inorg. Chem.* **1992**, 31, 303.

CHAPTER 2

VIBRATIONAL SPECTROSCOPY - A GENERAL INTRODUCTION

2.1 Vibrational Transitions

The vibrations of a diatomic molecule can be described most simply in terms of the harmonic oscillator approximation.¹⁻³ For a molecule AB of masses m_1 and m_2 , the harmonic oscillator has a parabolic potential well which relates the atomic displacements of atoms A and B from their equilibrium positions to the potential energy of the diatomic AB molecule. The discrete vibrational energy levels of the AB molecule are characterized in quantum mechanical terms by the vibrational quantum number v , as follows:

$$E_v = (v + 1/2)h\omega \text{ or } (v + 1/2)h\bar{\omega} \quad [2.1.1]$$

where $v = 0, 1, 2, 3$, etc., $\omega = h/2\sqrt{(k/\mu)}$, and $\bar{\omega} = h/2c\sqrt{(k/\mu)}$. The frequency (ω) and wavenumber ($\bar{\omega}$) of the harmonic vibration of the diatomic molecule are dependent on the force constant (k) and the reduced mass (μ), where $\mu = m_1m_2/(m_1 + m_2)$. The only allowed vibrational transitions are those between adjacent energy levels, i.e., $\Delta v = \pm 1$. Because real molecules are not strictly harmonic, the potential energy can be better approximated by the Morse function, for which the energy levels are now given by:

$$E_v = \bar{\omega}_e(v + 1/2) - \bar{\omega}_e x_e(v + 1/2) \quad [2.1.2]$$

where $\bar{\omega}_e$ is the wavenumber corrected for anharmonicity and $\bar{\omega}_e x_e$ is the actual anharmonicity. The energy levels of a Morse oscillator are not equidistant from one another; ΔE decreases as v increases. The transition from the $v = 0$ to the $v = 1$ state is known as the fundamental transition. Anharmonicity effects also lead to a breakdown in

the formal selection rule and so weaker overtone transitions such as those from $v = 0$ to $v = 2, 3, 4...$ etc. can now be detected. The smaller the x_e value the more the vibration behaves like a harmonic oscillator, while a larger x_e value implies considerable vibrational anharmonicity.

2.2 Infrared Absorption

When a molecule is irradiated with electromagnetic radiation of energy $h\nu$, the energy may be transmitted, absorbed, or scattered. From the classical description, IR absorption occurs when the molecular vibrational frequency corresponds to the frequency of the incident radiation, i.e.,

$$E_{\text{molecule}} = h\nu_{\text{vibration}} \quad [2.1.3]$$

In order to absorb IR radiation, a molecular vibration must lead to a change in the dipole moment of the molecule. Thus, a vibrating heteronuclear molecule will have an oscillating dipole. An applied oscillating field of electromagnetic radiation will induce a dipole, μ_{ind} , which will oscillate at the same frequency. At a certain frequency coincident with the molecular vibrational frequency, the dipole moment and the nuclei will oscillate simultaneously. At such a frequency, the change in dipole moment will allow a quantum of energy to be absorbed and a vibrational transition will be induced.

2.3 Raman Scattering

In Raman spectroscopy, the sample is irradiated with an intense source of monochromatic light, nowadays usually a visible light laser. Some of the emitted light is scattered inelastically. From classical theory,³ the Raman effect is dependent upon just

how much the polarizability of the molecule is changed during a molecular vibration. The induced dipole in this case is proportional to the electric field strength and is given by:

$$\mu_{\text{ind}} = \alpha E \quad [2.1.4]$$

where α is the molecular polarizability and E is the electric field strength. In molecules, the polarizability does not have a constant value - its magnitude will vary as the molecule vibrates. Thus, α will vary at the natural vibrational frequency of the bond and can be described as a function of the vibrational frequency:

$$\alpha = \alpha_0 + (\Delta\alpha)\cos(2\pi\nu_0 t) \quad [2.1.5]$$

where α_0 is the equilibrium polarizability, a second-order tensor, and α is the maximum amplitude, and ν_0 is the natural vibrational frequency. The energy of the oscillating electric field of the electromagnetic radiation can be given as $E = E_0 \cos(2\pi\nu t)$ and so equation [2.1.5] can be written as:

$$\mu_{\text{ind}} = \alpha_0 E_0 \cos(2\pi\nu t) + (1/2)\Delta\alpha E_0 [\cos 2\pi(\nu + \nu_0)t + \cos 2\pi(\nu - \nu_0)t] \quad [2.1.6]$$

Equation [2.1.6] indicates that the induced dipole moment will oscillate with components of frequency ν , $\nu + \nu_0$, and $\nu - \nu_0$ which will result in Rayleigh scattering (i.e., coincident with the incident radiation) and Stokes and anti-Stokes Raman scattering, respectively. The vibrational frequencies are observed as Raman shifts from the incident frequency. The Stokes bands on the low-energy side of the Rayleigh line are more intense than are the anti-Stokes bands since the former originate from the $\nu = 0$ ground state and most molecules are in this state at ambient temperatures. Equation [2.1.6]

corresponds to the quantum mechanical description for Raman transitions where $\Delta v = \pm 1$

2.4 Normal Modes of Vibration

Unlike diatomic molecules, which have a single fundamental vibration, polyatomic molecules with N atoms undergo much more complex vibrations. The motion of each atom has three independent degrees of freedom in the x , y , and z directions of a Cartesian coordinate system. These complex vibrations can be resolved into $3N-6$ degrees of freedom when the three translations and three rotations of the molecule as a whole are subtracted. It can be shown that these $3N-6$ internal degrees of freedom correspond to $3N-6$ internal normal modes of vibration. A linear polyatomic molecule has $3N-5$ since there is no rotation about the molecular axis.

In a normal coordinate analysis,^{4,5} the kinetic and potential energies of a molecular vibration are described using either Cartesian (q_k) or internal coordinates (S_k) which measure the displacement of each nuclear mass from its equilibrium position, or the changes in bond length or bond angle from the equilibrium values. A single normal coordinate Q can also define a normal mode of vibration. Combined with Newton's equation of motion, the mathematical solution to this vibrational problem is given by:

$$Q_i = Q_i^0 \sin(\lambda_i t + \delta_i) \quad [2.1.7]$$

The $3N$ coordinates are Q_i where $\delta_i = 1, 2, 3, \dots, 3N$, and Q_i^0 and δ_i are the amplitude and phase constants of the vibration, respectively, and $\lambda_i = 2\pi\nu_i$ which is characteristic of a simple harmonic motion with a frequency $\nu = \lambda/2\pi$. This means that each normal coordinate is vibrating with its own characteristic frequency ν_i . In order to depict atomic displacements during a vibration, the internal coordinates (S_k) are evaluated per unit change in the normal coordinate (Q_i) by means of a transformation matrix:

$$S_k = \sum B_{kj} Q_j \quad [2.1.8]$$

where B_{kj} is an appropriate coefficient. If only one normal coordinate Q_1 is excited, then:

$$S_k = B_{k1} Q_1 \sin(\lambda_1 t + \delta_1) = A_{k1} \sin(\lambda_1 t + \delta_1) \quad [2.1.9]$$

At this point, every internal coordinate of S_k will vibrate with the same phase constant (δ_1) and frequency (ν_1), and all the atoms will pass through the equilibrium position simultaneously. This situation describes a normal mode of vibration.

A set of linear homogeneous equations, called a secular equation, with an order of $3N-6$ can be derived for the $3N-6$ vibrations. For complex molecules where atomic displacements occur along the three Cartesian axes, the Wilson GF matrix method is applicable. The secular equation can be solved for the $3N-6$ characteristic values of λ . Each λ value is used to calculate the ratios of the amplitudes A_{k1} , A_{k2} , etc. Thus, each of the internal coordinates (S_k) vibrates with a relative amplitude of B_k proportional to the normal coordinate Q_1 . These values give the ratios of the displacements in the normal vibrations whose normal coordinates are Q_1 , Q_2 , etc. These displacements are sufficient to describe the normal modes of vibration. The atomic displacements of a normal vibration can then be drawn if the coordinate Q_1 is translated into a set of Cartesian coordinates where a unit change in the Cartesian coordinates, $q_k = x_N, y_N, z_N$, for each atom N is related to the internal coordinate by B_{kj} .

2.5 Vibrational Spectroscopy of Crystals

The $3N-6$ internal normal modes of vibration of an N -atom molecule can be classified into various species according to their symmetry properties.^{4,6} The number of

normal vibrations is equal the number of irreducible species of its point group. From group theory, the selection rules for the IR- and Raman-active vibrations depend upon these species belonging to one of the components of the dipole moment or polarizability, respectively. In the crystalline state, the symmetry of the molecule differs from that of the isolated state. This situation may result in splitting of some vibrations and activating any previously IR- or Raman-inactive bands in the spectra of the solid. In addition to the internal vibrations, the ensemble of translatory and rotatory vibrations of a crystal constitute the lattice (or external) modes, which are normally observed in the far-IR region. The vibrations are governed by a new set of selection rules based on the symmetry of the crystal concerned.

The symmetry of the crystalline field surrounding a molecule is characterized by the site group.⁷ A molecule occupies a given site group in a crystallographic unit cell. Thus, a site group is a subgroup of the space group and the molecular point group of a free molecule. The site group can only be the same as or of lower symmetry than that of the molecular symmetry. The symmetry of the lattice is further specified by the symmetry operations of the factor group which is a subgroup of the space group in which the translation operations are assigned to the identity operation. The distribution of vibrations among the factor group can be determined by a method called factor group analysis which incorporates the molecular point group, the site symmetry, the space group, and the number of molecules per primitive unit cell. Since the site group is a subgroup of both the factor group and the molecular point group, a correlation table between the different symmetries can be constructed for both the internal and external vibrations. The optically-active vibrations of a crystal (both internal and external) can be described by the irreducible representations from the site and factor group correlations. The symmetries of the external vibrations are given by the irreducible representations of the molecular point group corresponding to the three translations (T_x , T_y , T_z) and three rotations (R_x , R_y , R_z).

Any correlation (or Davydov) splitting resulting from the loss of vibrational degeneracy of the internal and external vibrational modes can be explained on the basis of an analysis of the site and factor group symmetries. The following factor group analysis of Zeise's anion $[(C_2H_4)PtCl_3]^-$ will illustrate the procedure.

2.6 Factor Group Analysis - Zeise's Salt

From an X-ray crystallographic study,⁸ Zeise's salt crystallizes in a monoclinic lattice of space group $P2_1/c$ (C_{2h}) with four molecules per unit cell ($Z = 4$). The site group can be found from the Halford tables,^{9,10} which give complete lists of the possible site symmetries and the number of equivalent sites for the 230 crystallographic space groups. For C_{2h} symmetry, there are three possible site symmetries: $C_1(4)$, $2C_2(2)$, and $4C_1(2)$. Since the number of equivalent sites must be equal to the number of molecules in the unit cell, only $C_1(4)$ is possible. The rotational axis of the four molecules is coincident with the rotational axis of the unit cell. The molecular point group of Zeise's salt is C_{2v} and the factor group symmetry is isomorphous with the space group C_{2h} . The C_1 site group is a subgroup of both the molecular point group (C_{2v}) and the factor group (C_{2h}). The ten atoms of Zeise's anion $[(C_2H_4)PtCl_3]^-$ result in $3(10)-6 = 24$ normal modes which are represented by:

$$\Gamma_{\text{vib}} = 8a_1 + 4a_2 + 6b_1 + 6b_2 \quad [2.1.10]$$

These symmetry species are all Raman active and, except for the a_2 modes, they are also IR active. The 24 internal vibrations can then be classified into the various symmetry species of the C_{2h} factor group by correlation through the C_1 site group. The correlation diagram is shown in Figure 2.1.1. In addition, there are $4(6)-3 = 21$ external optical vibrations or lattice modes. A factor group analysis of the entire primitive cell, including

counter ions, is necessary to account for the external modes. This part of the factor group analysis will not given here since these external modes are only observed at very low frequencies (usually $< 120 \text{ cm}^{-1}$) and no definite assignments have been made for Zeise's salt for any bands that appear below 300 cm^{-1} .

Figure 2.1.1 Factor Group Splitting for Zeise's salt.

Molecular point group symmetry	Site group symmetry	Factor group symmetry
C_{2v}	C_1	C_{2h}
8a ₁ (IR,R)	24a (IR,R)	24b _g (R)
4a ₂ (R)		24b _g (R)
6b ₁ (IR,R)		24b _u (IR)
6b ₂ (IR,R)		24b _u (IR)

From the correlation table, there are two effects of the crystal symmetry on the selection rules governing molecular vibrations. First, there is the site symmetry effect which, in this case, results in lowering of the spectroscopic symmetry from C_{2v} to C_1 . As a result, all four of the originally optically-inactive a₂ vibrations now become IR- and Raman-active. Since a non-centrosymmetric symmetry is preserved, the rule of mutual exclusion is not applicable. The second effect is that the crystal structure results in the possibility of vibrational coupling between the four molecules in the unit cell. Each of the 24a vibrations in the site group could be split into two sets of doublets in the factor group. One set is the Raman-active species ($24a_g + 24b_g$), while the other is the IR-active species ($24a_u + 24b_u$). Therefore, correlation to the centrosymmetric factor group

should cause each component of the site group to be split into four components. The crystal could therefore exhibit 48 Raman and 48 infrared non-coincident bands.

2.7 Pressure Effects on Crystals

Spectroscopic experiments performed as a function of applied pressure monitor the effects of changes in the intra- and intermolecular interatomic distances.¹¹

The anharmonicities of these interactions produce changes in the internuclear spacings which subsequently induce changes in the force constants. As a result, the vibrational frequencies are pressure dependent and can be represented by $d\nu/dp$.

The frequency shifts induced by the pressure changes do not effect the form of the normal coordinates and so the form of the vibrations remains unchanged. Force constants are significantly affected by vibrational anharmonicities, even when only small displacements in the intra- and intermolecular bond lengths are involved. The extent of anharmonicity in a force constant can be expressed in terms of a percentage change in force constant with respect to a percentage change in bond length.¹² The equation for a small displacement, x , in an external mode of vibration is:

$$k/k_0(100) = -100(n + m + 3)/r_e \quad [2.1.11]$$

where r_e is the equilibrium bond length, $\Delta k = (k - k_0)$ is the difference in force constants arising from the nuclear displacements, and n and m are constants. On the basis of this model, it has been found that all bond stretching force constants are anharmonic and, even for strong covalent bonds, there is about a 6% increase in k for a 1% decrease in r . The rate of frequency shift with applied pressure ($d\nu/dp$) is also volume dependent. This contribution can be estimated from the Grüneisen parameter,¹³ which is given by:

$$\gamma = -d(\ln \nu_i)/d(\ln V) = -(V/\nu_i) d(\nu_i/dV) \quad [2.1.12]$$

The $d\nu/dp$ data obtained from the high-pressure spectroscopic measurements can be used to determine γ , using the following equation:

$$\gamma \kappa_v = (d\nu/dp)T \quad [2.1.13]$$

where κ_v is the isothermal compressibility of the crystal.

The pressure-induced frequency shifts of the IR and Raman bands usually give γ values within the range of 0.03 to 3.0. When pressure is applied to a crystal, it is the intermolecular bonds that decrease more easily to cause most of the volume change; the intramolecular bond lengths, which have higher repulsive forces, are only slightly affected. Therefore, the smaller γ values are more representative of the internal vibrational modes.

REFERENCES

- (1) Herzberg, G. *Molecular Spectra and Mol. Structure Vol 1. Spectra of Diatomic Molecules*; 2 ed.; Van Nostrand Reinhold Co.: New York, 1950.
- (2) Potts, W. J. *Chemical Infrared Spectroscopy*; J. Wiley: New York, 1963; Vol. 1.
- (3) Harris, D. C.; Bertolucci, M. D. *Symmetry and Spectroscopy. An Introduction to Vibrational and Electronic Spectroscopy*; Dover, 1978.
- (4) Wilson, E. B.; Decius, J. C.; Cross, P. C. *Molecular Vibrations*; Maple Press Co.: 1955.
- (5) Nakamoto, K. *Infrared and Raman Spectra of Inorganic and Coordination Compounds*; 4 ed.; Wiley-Interscience: New York, 1986.
- (6) Turrell, G. *Infrared and Raman Spectra of Crystals*; Academic Press: 1972.
- (7) Fateley, W. G.; Dollish, F. R.; McDevitt, N. T.; Bentley, F. F. *Infrared and Raman Selection Rules for Molecular and Lattice Vibrations*; Wiley-Interscience: New York, 1976.
- (8) Love, R. A.; Koerzle, T. F.; Williams, G. J. B.; Andrews, L. C.; Bau, R. *Inorg. Chem.* **1975**, 14, 2653.
- (9) Halford, R. S. *J. Chem. Phys.* **1946**, 14, 2653.
- (10) Adams, D. M. *Metal Ligand and Related Vibrations*; E. Arnold Press Ltd.: 1966.
- (11) Ferraro, J. R. *Vibrational Spectroscopy at High External Pressures*; Academic Press: 1984.
- (12) Herzberg, G. *Molecular Spectra and Mol. Structure Vol II. Infrared and Raman Spectra of Polyatomic Molecules*; D. Van Nostrand Co.: Princeton, 1945.
- (13) Zallen, R. *Phys. Rev.* **1974**, B9, 4485.

CHAPTER 3

EXPERIMENTAL

3.1 High-pressure Infrared Spectra

Infrared spectra were measured on a Nicolet 6000 FT-IR spectrometer equipped with a liquid nitrogen-cooled mercury cadmium telluride (MCT-B) detector. The IR diamond-anvil cell (DAC) from Diamond Optics Inc. (Tucson, Arizona) was equipped with a pair of type-IIA diamonds. The 2600-1800 cm^{-1} optical region was obscured by an intense diamond absorption. Stainless-steel gaskets, 200 μm in thickness with a hole 400 μm in diameter, were placed between the parallel diamond faces. The pressure calibrant used was sodium nitrite (NaNO_2) diluted in a NaBr matrix (0.3-0.5 wt%), stored at 180°C. In all the pressure experiments, the antisymmetric stretching mode [$\nu_a(\text{NO}_2)$] at 1279 cm^{-1} and with a half-bandwidth of 25 cm^{-1} at ambient pressure was monitored. Although sodium nitrate (NaNO_3) is usually employed as the IR pressure calibrant, under the conditions of our experiments there was considerable overlap between the calibrant band [$\nu_a(\text{NO}_3)$] at 1401 cm^{-1} and the sample absorption bands. On the other hand, using NaNO_2 resulted in no significant overlap at any pressure. The equation used to calculate the pressure on the sample was:¹

$$p = 2.356\Delta\nu - 1.334 \nu \exp(-\Delta\nu/92) \quad [3.1.1]$$

where ν is the measured peak shift in wavenumbers (cm^{-1}) at each pressure from the atmospheric pressure value.

The DAC was loaded as follows. With the gasket placed over the lower diamond face, held down by plasticine, a small piece of calibrant was placed into the gasket hole with the aid of an optical microscope and then pressed slightly to form a uniform layer.

The cell was reopened and the sample was packed into the hole. After the cell was reassembled, just enough pressure was applied to form a transparent layer. The pressure was then released and the system was allowed to equilibrate for a few hours. The DAC was then mounted onto an x-y-z stage together with a Spectra-Bench 4X beam condenser and aligned in the IR spectrometer for maximum absorption intensity. Infrared spectra were recorded at intervals of 1-3 kbar. The resolution was typically 2 or 4 cm^{-1} and usually 500 scans were coadded. An equilibration time of at least 30 min was necessary between each pressure change, prior to recording the spectrum, or else the nitrite calibrant absorption band tended to split. This splitting was most probably due to an uneven distribution of hydrostatic pressure and a slow rate of pressure equilibration throughout the calibrant.

3.2 High-pressure Micro-Raman Spectra

Raman spectra were recorded on an Instruments S. A. spectrometer with a Jobin Yvon Ramanor U-1000 double monochromator equipped with a Nachet optical microscope, interfaced to an IBM PS/2 model 60 computer for data collection and processing. The excitation sources used were the 514.532-nm line of a Spectra Physics model 164, 5-W argon-ion (Ar^+) laser and a 568.188-nm line of a Coherent Innova 100-K3, 3W krypton-ion (Kr^+) laser for $\text{Pt}(\text{COD})\text{Cl}_2$ and $\text{K}[(\text{C}_2\text{H}_4)\text{PtCl}_3]$, respectively. Slit widths of typically 300 and 500 μm were used yielding resolutions of 2 and 4 cm^{-1} , respectively.² The DAC was purchased from Diacell Products (Leicester, England) and was equipped with type IIA diamonds. A stainless-steel gasket, 400 μm thick, with a 300 μm diameter hole, was placed between the parallel diamond faces. The sample, together with a ruby chip as the pressure calibrant, was placed inside the hole. The DAC was mounted on the x-y stage under the 4X objective of the microscope. The ruby

fluorescence was scanned before and after each sample scan and the pressure was calibrated with the ruby R_1 line according to the following equation:³

$$p = -1.328\Delta\bar{\nu} + 0.0003(\Delta\bar{\nu})^2 \quad [3.1.2]$$

where $\Delta\bar{\nu}$ is the observed shift in the ruby R_1 fluorescence band from its position at atmospheric pressure; viz., 5029.6 cm^{-1} for Ar^+ and 1048.1 cm^{-1} for Kr^+ . The high-pressure spectra were measured every 1-4 kbar upon compression. For Zeise's salt, a 3-point spectral smoothing was applied to the data. The linear pressure dependences ($d\nu/dP$) of the observed vibrational modes were calculated by means of a linear least-squares treatment of the plots of the peak positions (cm^{-1}) versus the applied external pressure (kbar). Straight-line plots were obtained with correlation coefficients of 0.95 or better.

3.3 Sample Source and Purity

The dehydrated Zeise's salt, $\text{K}[\text{Pt}(\eta^2\text{-C}_2\text{H}_4)\text{Cl}_3]$ (Aldrich Chemical Co.: purity 99%), Zeise's dimer, $[(\text{Pt}(\eta^2\text{-C}_2\text{H}_4)\text{Cl}_2)_2]$ (Strem Chemicals Inc.: purity 99%), and dichloro(1,5-cyclooctadiene)platinum(II), $[\text{Pt}(\text{COD})\text{Cl}_2]$ (Strem Chemicals Inc. purity: 99.5%) were obtained from the sources indicated. The purity of each compound was checked by melting point measurements; the m.p.'s were all within $\pm 2^\circ \text{C}$ of the literature values. All samples were used without further purification.

References

- (1) Klug, D. D and Whalley. E. Rev. Sci. Instrum. **1983**, 54, 1205.
- (2) Piermarini, G. J; Block, S.; Barrett, J. D and Formans, R.A. J. Appl. Phys, **1975**, 46, 2774.

CHAPTER 4.

SPECTROSCOPIC STUDIES ON ZEISE'S SALT :K [Pt(η^2 -C₂H₄)Cl₃]

4.1. Vibrational Assignments

The vibrational spectrum of Zeise's salt, K[(η^2 -C₂H₄)PtCl₃], has been widely investigated,^{1-10,11} chiefly with the aim of identifying the vibrational modes of the platinum-ethylene moiety. The use of certain vibrational frequencies as indicators of the extent of metal-olefin interactions has been hindered by disagreements concerning the correct assignments of the vibrational modes, particularly the C=C stretch in Zeise's salt. The difficulties arise as a result of extensive mixing of the internal coordinates of the normal modes, especially those which involve the C=C stretching and the symmetric CH₂ deformation motions. In addition, the ethylene ligand is symmetrically bound to the metal and the weak C=C stretch is difficult to detect by IR spectroscopy. Since both the C=C bond stretching and the in-plane CH₂ deformation modes in Zeise's salt have a₁ symmetry and similar frequencies, these vibrations are strongly coupled. The vibrational modes in Zeise's dimer, [(η^2 -C₂H₄)PtCl₂]₂, are similar to those in Zeise's salt. A survey of the literature shows that very few spectroscopic data are available for the dimer.^{2,4}

The earliest systematic studies of Pt-olefin complexes were carried out by Chatt and Duncanson,¹² who assigned bands in the 1500 cm⁻¹ region to the C=C stretch. Many platinum(II) complexes coordinated with higher olefins, where there is no CH₂ coupling, show a band at ~1500 cm⁻¹ which has been assigned to ν (C=C), providing strong support for this assignment in Zeise's salt. More recently, complete assignments have been proposed for the whole molecule, its deuterated analogue, and the related dimer.²⁻⁴ Hirashi's assignments were based on the metallopropane model,³ and affords the most complete vibrational data available. Assignments have been given for both the solid and solution spectra, including Raman polarization measurements. Two bands were assigned

to the coupled C=C stretch, at 1515 and 1240 cm^{-1} , the latter containing more C=C stretching character. Two Pt-olefin vibrational bands were also assigned. The metallopropane model, which implies both strong σ - and π -interactions between the Pt and the ethylene, has been accepted by some authors.^{7,12,13} On the other hand, Grogan and Nakamoto³ have assigned only one band to the Pt-olefin stretch and have attributed the C=C stretching mode (with some contribution from CH₂ scissoring) to the a band at 1516 cm^{-1} . From the associated potential energy distribution, the CH₂ scissoring mode at 1416 cm^{-1} is strongly coupled to the C=C stretch. This alternative model implies a σ -bonded Pt-olefin system with a minimal contribution from π -bonding. Jobic's⁵ vibrational assignments on the basis of inelastic neutron scattering data for the a_1 and b_1 modes of the C_{2v} symmetry $[(C_2H_4)PtCl_3]^-$ anion are in reasonable agreement with those of Hirashi. However, Jobic concluded that the σ -bonding interaction was more important than was π -backbonding. The most recent vibrational analysis on Zeise's salt using FT-IR and FT-Raman spectroscopy by Mink et al.¹¹ suggests some modifications to the previously accepted assignments. Three polarized Raman lines for $Pt(C_2H_4)_3$ were assigned to the coupled C=C stretching and deformation modes. Likewise, three sets of polarized frequencies in Zeise's salt were assigned to the strongly coupled $\nu(C=C)$ stretch, CH₂ scissoring and CH₂ wagging modes at 1525, 1415 and 1253 cm^{-1} respectively. However, the vibrational modes with a higher component of $\nu(C=C)$ stretch were left unassigned. The two extreme bonding situations from the above vibrational assignments suggest that the actual hybridization¹⁴ for the ethylene carbons is in between sp^2 and sp^3 . Clearly, assignment of either band to purely C=C stretching is not justified, and so no correlation can be made between the lowering of the C=C frequency on coordination and the extent of C=C bond weakening.¹⁵ Similarly, the strength of the Pt-olefin bond cannot be estimated by the shift of the associated vibrational mode. In view of the difficulty in assigning the different modes, the extent of olefin perturbation upon coordination has been estimated by comparing the frequencies of free and coordinated

C_2H_4 , its deuterated analogue,^{2,3} and also by the sum of the percentage lowering of the C=C stretch and $\delta(CH_2)$ modes.⁷ The frequency shifts upon coordination are small except for the $\nu(C=C)$, $\delta(CH_2)$, and CH_2 twist modes. This approach agrees well with other measurements such as the upfield ^{13}C -NMR chemical shifts and $J(^{195}Pt-^{13}C)$ coupling constants.¹⁶ Of course, the estimated shifts of the vibrational modes are highly dependent on the particular vibrational assignments chosen and so the results vary quite widely.

The symmetric and antisymmetric Pt-ethylene stretching modes in Zeise's salt have generally been assigned to bands appearing at 405 and 493 cm^{-1} , but again both frequencies contain significant contributions from other vibrational modes.³

As mentioned already, a number of force field calculations have been performed for Zeise's salt.^{1-5,9,17} The resulting force constants are not really comparable, however, because either different models were used for the internal coordinates or some of the vibrational frequencies were assigned incorrectly. In all of the normal coordinate treatments, it was assumed that there is no vibrational coupling between the ethylene and the $PtCl_3$ moiety. The stretching force constants reported by Jobic⁵ and Hirashi³ using the same model are in reasonable agreement. Grogan and Nakamoto² used a point mass model for ethylene in the anion and treated the ethylene moiety separately. A comparison of the force constants for coordinated and free ethylene reveals that the greatest changes upon coordination occur, not surprisingly, in the CH_2 scissoring, C=C stretch, and CH twisting force constants.^{2,3,5} These force constants decrease upon coordination, indicating a reduction in the C=C bond order due to π -backbonding. This bond order lowering and the relative extents of σ and π bonding have been the subject of much discussion (*vide supra*, Chapter 1). With the considerable amount of conflicting vibrational data available on Zeise's salt, an accurate assignment of all the vibrational modes is not trivial. The assignments used in the high-pressure studies of Zeise's salt and

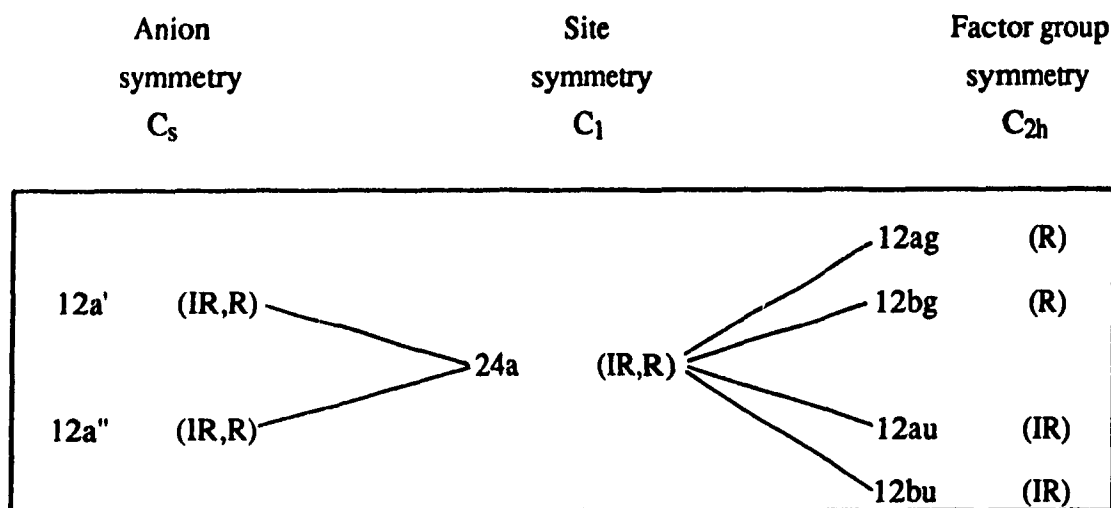
the related dimer to be described below were based chiefly on those given by Grogan and Nakamoto,² and Hirashi.³

It will be shown that some of the previously questionable assignments can now be made with much greater confidence as a result of the high-pressure work.

4.2 Solid State Symmetry

The crystallographic space group of Zeise's salt is $P2_1/c$ (C_{2h}) with four molecules per unit cell. There are 24 normal modes of vibration for the isolated C_{2v} -symmetry anion which are all both IR and Raman active, with the exception of the four a_2 modes which are IR inactive. A factor group analysis relating the C_{2v} molecular symmetry and the C_{2h} crystal symmetry is shown in Figure 2.1.1. The C_{2h} group is centrosymmetric and so the rule of mutual exclusion should apply. Owing to the small number of Raman bands observed, however it proved difficult to establish the presence or absence of any coincidences in the IR and Raman spectra. Correlation splitting would be expected in both the solid-state IR and Raman spectra.

On the basis of earlier X-ray data, the anion was shown to slightly distorted and should perhaps be treated in terms of C_s rather than C_{2v} symmetry.⁶ The factor group analysis for such a C_s symmetry is given in Figure 4.1.1. This analysis results in the same spectral predictions for crystalline Zeise's salt as does that for the C_{2v} anion (Figure 4.1.2). It should be mentioned here that the salt has recently been re-examined by neutron diffraction¹⁸ and the distortion from ideal C_{2v} symmetry is even less than was originally thought. The mid-point of the C=C bond and the Pt atom are 0.22 and 0.03 Å above the PtCl₃ plane, respectively. The C=C bond makes an angle of 5.9° with the normal to this plane. In view of these results, the symmetry of the anion was considered to be C_{2v} for the purposes of the high pressure work.

Figure 4.1.1 Factor Group Splitting for Zeise's Salt.

4.3 High Pressure Effects

Details of the IR and Raman bands observed for Zeise's salt at ambient pressure are given in Tables 4.1.1 and 4.1.2, respectively. The pressure dependences of vibrational modes were obtained from the slopes of the linear fits of the band positions versus the applied external pressures. The resulting pressure dependences ($d\nu/dp$) and relative pressure dependences ($d \ln \nu/dp$) are also given in these tables. Figures 4.1.2 and 4.1.3 show the frequency versus pressure plots for the IR-active modes up to 31.4 kbar and Raman-active modes up to 33.2 kbar, respectively. Figures 4.1.4 and 4.1.5 illustrate the far- and mid-IR spectra at ambient pressure. The lattice modes below 125 cm^{-1} could not be measured because they were obscured by the diamond fluorescence. The absence of any breaks in the slopes of the plots indicates that there were no pressure-induced phase changes throughout the pressure range investigated.

In general, most bands shift to higher wavenumbers with increasing pressure as a result of anharmonicities in the potential functions and also because application of

external pressure to a crystal lattice compresses the unit cells thereby resulting in increases in the vibrational force constants. The latter effect occurs because the interatomic and intermolecular interactions increase as the separations decrease.¹⁹ The $d\nu/dp$ values reported for most internal stretching modes range typically from 0.3 to 0.8 $\text{cm}^{-1} \text{kbar}^{-1}$. Any abnormal behaviour such as very large, small or even negative pressure dependences must be discussed in terms of (1) the particular chemical bond involved, (2) the nature of the vibrational mode concerned (stretch, bend, etc.), and (3) the importance of any intra- and intermolecular interactions.^{20,21}

The pressure dependences of the Pt-Cl and Pt-C₂H₄ stretching modes in Zeise's salt are higher than those for the C-H stretches of the C₂H₄ moiety. An early high-pressure study²² on non-cubic K₂[PtCl₄], in which crystallographic axes $a_0 = b_0 = c_0$, revealed that the most pressure sensitive vibrational mode was the translatory lattice mode along the longer a_0 axis, while the least sensitive was along the shorter c_0 axis. It is quite possible, therefore, that the monoclinic unit cell of Zeise's salt may also have vibrational modes which display different pressure sensitivities from others.

(i) C-H Stretching Region

The pressure dependences for the antisymmetric [$\nu_a(\text{C-H})$] and symmetric [$\nu_s(\text{C-H})$] modes generally have high pressure dependences.¹⁹ Although the bonds are stronger and consequently more difficult to compress, they are shorter and a small decrease in length will be high in terms of percent decrease. Another contribution to the high pressure dependences is that vibrations involving hydrogens are the most anharmonic.

TABLE 4.1.1. Pressure Dependences of Infrared Peaks of Zeise's Salt.

ν (cm^{-1})	$d\nu/dp$ ($\text{cm}^{-1}\text{kbar}^{-1}$)	$d \ln\nu/dp$ ($\text{kbar}^{-1}\times 10^2$)	Assignment ^a	Assignment ^b
3093	0.68	0.021		$a_2, \nu_s(\text{C-H})$
3075	0.64	0.020		$b_2, \nu_a(\text{C-H})$
3010	0.38	0.012	$b_1, \nu(\text{CH}_2)$	$a_1, \nu_s(\text{C-H})$
1418	-0.08	-0.0056	$a_1, \delta_s(\text{CH}_2)$ + $\nu(\text{C=C})$	$a_1, \delta_s(\text{CH}_2)$ + $\nu(\text{C=C})$
1252	0.37	0.029	$a_1, \rho_r(\text{CH}_2)$	$a_1, \nu(\text{C=C})$ + $\delta_s(\text{CH}_2)$
1192	0.17	0.014		$b_2, \rho_t(\text{CH}_2)$
1033	0.27	0.026	$b_1, \rho_w(\text{CH}_2)$	$b_1, \rho_w(\text{CH}_2)$
1025	0.16	0.015	$b_2, \rho_w(\text{CH}_2)$	
736	0.54	0.073	$a_1, \rho_t(\text{CH}_2)$	$b_1, \rho_r(\text{CH}_2)$
490	0.72	0.14		$b_1, \nu_a(\text{Pt-C}_2\text{H}_4)$

^a From Grogan and Nakamoto ref. 2. ^b From Hiraishi ref. 3.

Table 4.1.2. Pressure Dependences of Raman Peaks in Zeise's Salt.

ν (cm^{-1})	$d\nu/dp$ ($\text{cm}^{-1}\text{kbar}^{-1}$)	$d \ln \nu/dp$ ($\text{kbar}^{-1} \times 10^2$)	Assignments ^{a,b}
490	0.76	0.15	$\nu_s(\text{Pt-C}_2\text{H}_4)^{a,b}$
396	0.66	0.16	$\nu_a(\text{Pt-C}_2\text{H}_4)^b$
336	0.59	0.17	$\nu_s(\text{Pt-Cl}_2)^{a,b}$
294	0.56	0.17	$\nu(\text{Pt-Cl}_t)^{a,b}$
213	0.72	0.033	skeletal def. ^a
182	0.39	0.021	

^a From Grogan and Nakamoto ref..2. ^b From Hiraishi ref. 3.

For symmetric vibrations, a change in molecular volume is possible, whereas for antisymmetric vibrations the volume should remain rather constant.²¹ Thus, it would be expected that, at higher pressures, the symmetric C-H stretching mode would be more affected than is the antisymmetric mode, as is the case in Zeise's salt. On the basis of the measured $d\nu/dp$ values, the previously arbitrary symmetry assignments given for the C-H stretches at ambient pressure are now confirmed as being $3093/3072 \text{ cm}^{-1}$ for the symmetric and 3010 cm^{-1} for the antisymmetric vibrations, respectively.

(ii) C=C Stretch

In ethylene, the vibrational modes which shift the most and show significant decreases in force constant upon coordination to a platinum atom are the $\nu(\text{C}=\text{C})$, the strongly-coupled CH_2 scissoring, and the CH_2 twisting (also known as C=C torsion) mode.^{2,3,5} Among these modes there is a wide variation in $d\nu/dp$ values. The coupled $\nu(\text{C}=\text{C})$ stretching mode has been assigned to the peak at 1253 cm^{-1} by Hiraishi.³

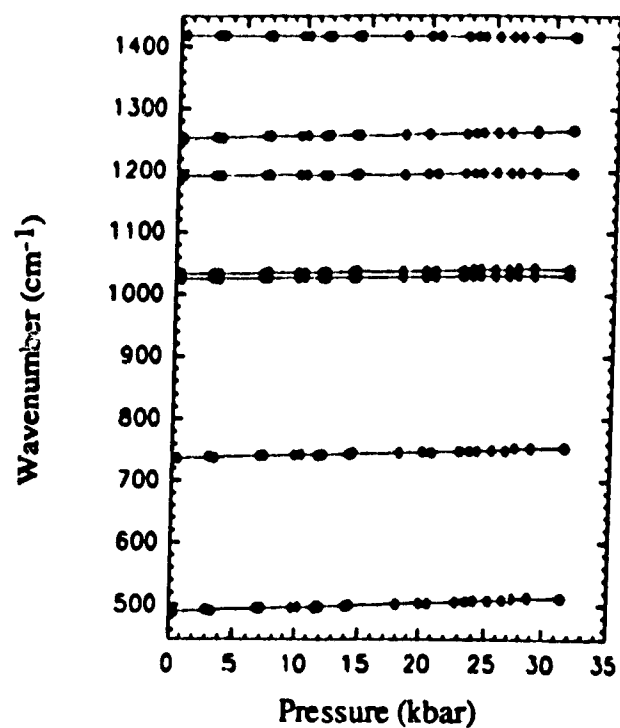


Figure 4.1.2 Pressure dependences of selected IR bands of Zeise's salt

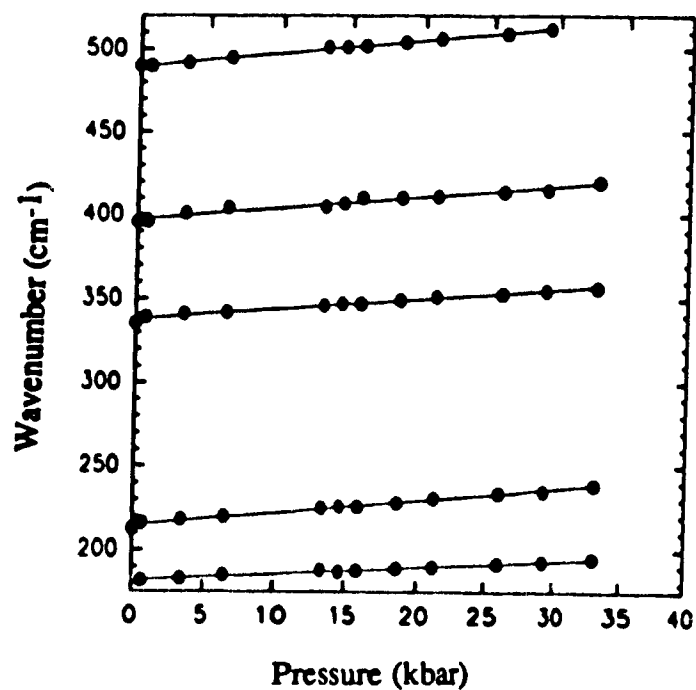


Figure 4.1.3 Pressure dependences of the Raman bands of Zeise's salt.

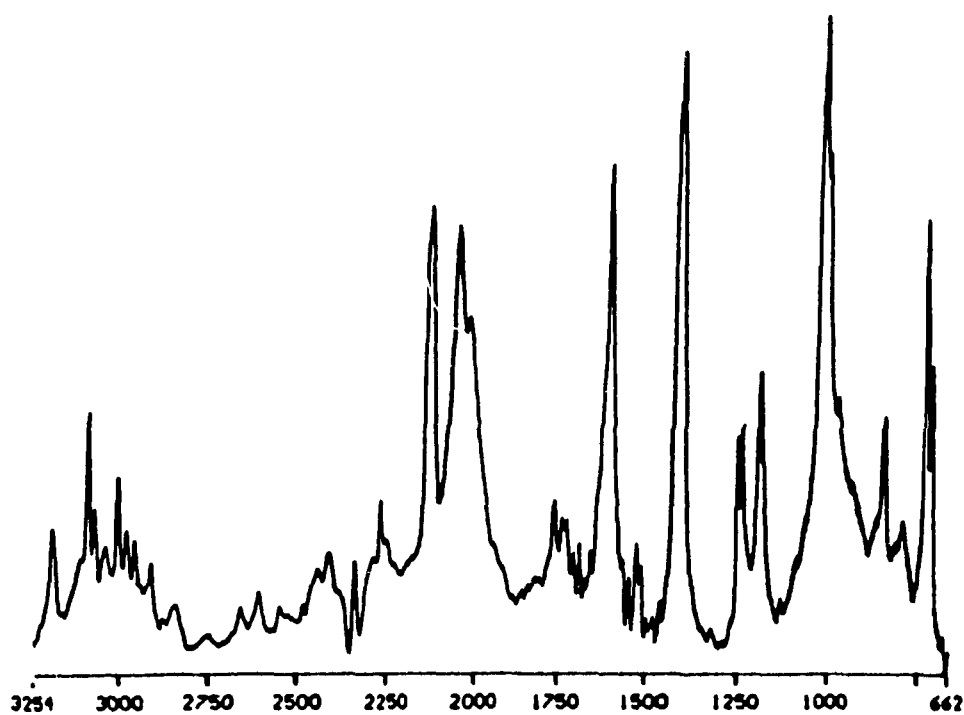


Figure 4.1.4 IR spectrum of Zeise's salt at ambient pressure

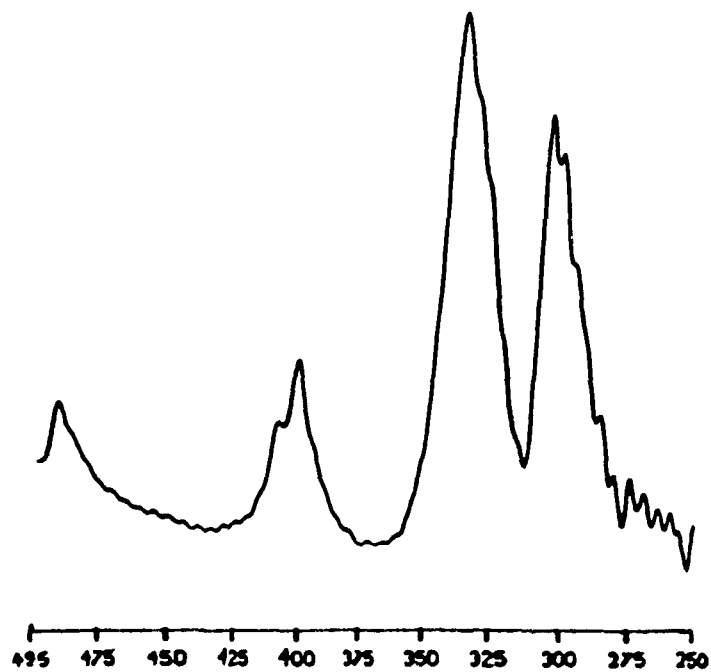


Figure 4.1.5 Far-IR spectrum of Zeise's salt at ambient pressure (x4 times weaker than the mid-infrared region).

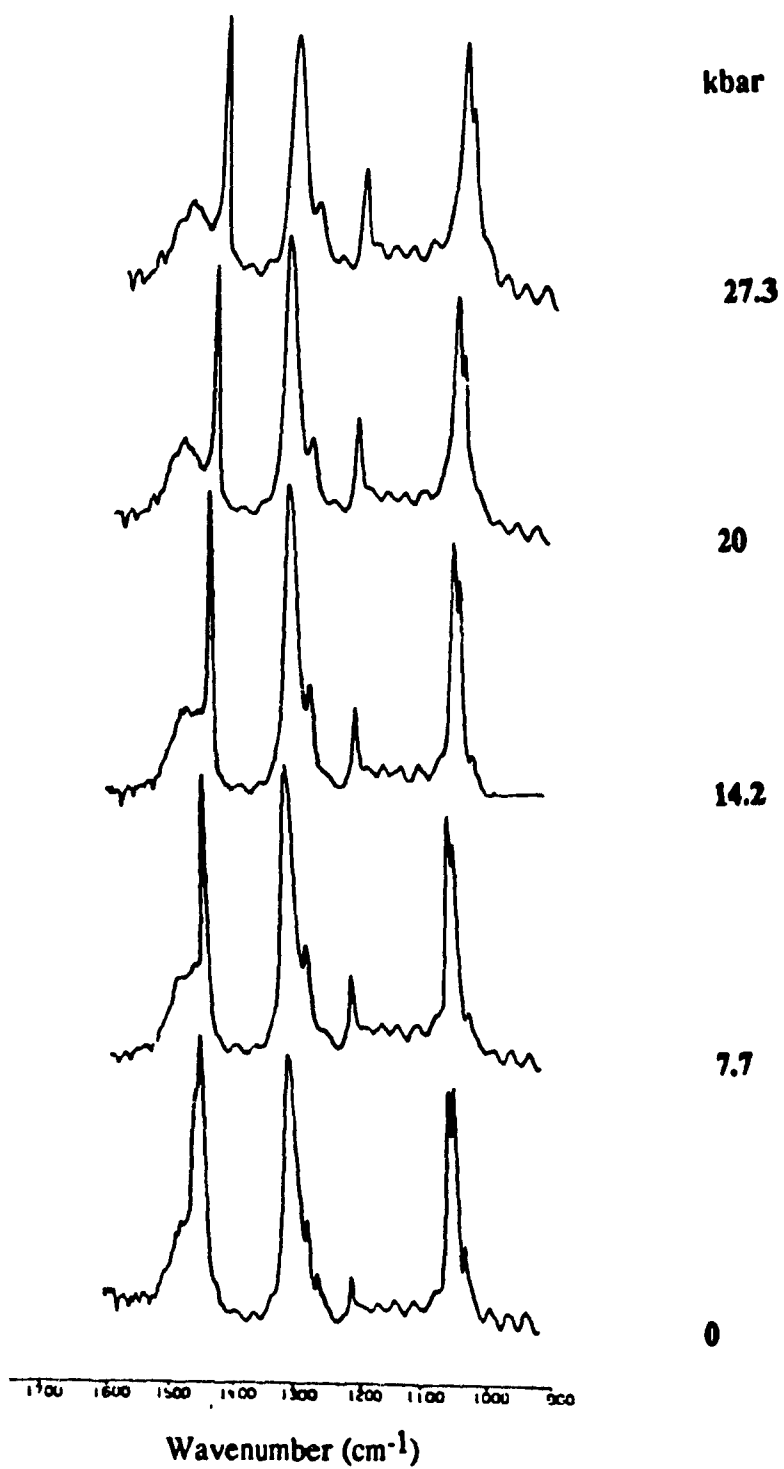


Figure 4.1.6 IR spectra of Zeise's salt at the indicated pressures upon compression.

His assignment was based on the observation of an intense polarized band in the solution Raman spectrum. Under pressure, this Raman band lost intensity appreciably at ~ 15.9 kbar and its position could not be measured accurately. This intensity decrease was chiefly due to overlapping with the intense, broad diamond fluorescence band at 1353 cm^{-1} . A C=C stretch at 1253 cm^{-1} (lowered by 370 cm^{-1} from free ethylene), situated between those normally found for alkane and alkene C=C stretches, implies the formation of a very strong Pt-olefin π -bond and a change in the hybridization of the ethylene carbons towards sp^3 . In the IR spectrum under pressure, however, this 1253 cm^{-1} band is apparently little affected by any increased π -backbonding and retains a positive $d\nu/dp$ value ($0.37\text{ cm}^{-1}\text{ kbar}^{-1}$). The positive pressure dependence may be exaggerated somewhat by the close proximity of the calibrant peak at 1279 cm^{-1} , but these peaks separate more at higher pressures due their different pressure dependences. On the other hand, according to Grogan and Nakamoto², the band at 1418 cm^{-1} should be assigned to the symmetric CH_2 scissoring mode coupled to the C=C stretch. Under pressure, this band displays a slight negative pressure dependence ($-0.08\text{ cm}^{-1}\text{ kbar}^{-1}$) which can be explained by using the argument put forward by Adams and Ekejiuba,²³ that pressure enhances the π -backbonding between a transition metal and a π -bonded ligand resulting in an unchanged or, as in this case, a decreased $\nu(\text{C}=\text{C})$ value. Figure 4.1.6 shows the mid-IR spectra observed at various pressures. The pressure dependence of the C=C stretching mode is the result of a number of competing factors. (1) Compression of the lattice will tend to shorten all of the intramolecular distances and consequently result in an increase in the vibrational energies of all the internal modes; (2) The increasing pressure strengthens the Pt-olefin π -backbonding leading to a reduction in bond order and a concomitant decrease in $\nu(\text{C}=\text{C})$; (3) There is an appreciable mixing between the C=C stretch and the CH_2 scissoring mode. Both of these modes are totally symmetric a_1 species which involve larger volume changes and thus more positive pressure dependence

would prevail. In the present case, there is apparently sufficient increase in the Pt-olefin π -backbonding with increasing pressure to counteract the opposing factors. Therefore, because of its pressure behavior the 1418 cm^{-1} band has been assigned to the $\nu(\text{C}=\text{C})$ mode. The other weak vibrational mode with a $\nu(\text{C}=\text{C})$ component at 1515 cm^{-1} collapsed in the IR spectrum under initial pressure application. The estimated extent of the CH_2 deformation coupling contribution within the $\text{C}=\text{C}$ modes has been heavily disputed.^{2,3,7} However, the pressure shift of a vibration is modified in both sign and magnitude by its selective coupling.²⁴ Therefore, the pressure dependence could be used as a tool to show the contribution of a π -bonded $\text{C}=\text{C}$ vibrational mode to a coupled band. The vibrational mode containing the larger $\nu(\text{C}=\text{C})$ component would be expected to have a more negative (or lower) $d\nu/dP$ value. In general, intensity changes can be used as an indication of the extent of vibrational coupling. In the case of polymethylene, Ley and Drickamer^{25,26} have reported a combined intensity increase for the $\text{C}-\text{C}$ stretching and the CH_2 wagging modes as the intermolecular coupling was increased by pressure. No relative intensity changes occurred for the bands at 1418 and 1252 cm^{-1} , and there were no peak splittings. These results indicate that there was either no coupling or no detectable change in the magnitude of coupling between these modes.

(ii) Pt-ethylene Stretches

The $\text{Pt}-\text{C}_2\text{H}_4$ group gives rise to two bands in the $550\text{-}400\text{ cm}^{-1}$ region in the Raman spectrum. These bands decrease in intensity with increasing pressure, and both bands display shoulders which later disappear as the bands broaden. The shoulders could be attributable to factor group splitting ($a_g + b_g$) modes. Both the symmetric and antisymmetric $\text{Pt}-\text{C}_2\text{H}_4$ stretches exhibit large pressure dependences. Similar large pressure dependences of the symmetric $\text{M}-\text{C}=\text{O}$ bond stretches found in other π -bonded systems by Huang et al.^{21,27-29} have been related to strengthening of the π -backbonding.

The pressure dependence for the symmetric Pt-C₂H₄ stretch (0.72 cm⁻¹ kbar⁻¹) is similar to the dv/dp values observed for these M-C=O systems (0.76-0.99 cm⁻¹ kbar⁻¹).

(iv) CH₂ Deformations

The CH₂ deformations of the ethylene moiety are also coupled. Most of the CH deformations, as expected, are less pressure sensitive than the stretching vibrations.²⁴ The effective volume change in these vibrational modes is small and consequently they have low pressure dependences and small $d \ln \nu / dp$ values. The symmetric CH₂ twist at 736 cm⁻¹, assigned by Nakamoto² and Jobic,⁵ has the largest dv/dp value, 0.54 cm⁻¹ kbar⁻¹, among the CH₂ deformations. This mode is dependent on the strength of coordination and is lower than the wagging and rocking modes as it weakened significantly.⁵ Hence, a more positive pressure dependence results. This band is coupled to a CH₂ rocking mode which appears as a weak broad band at 840 cm⁻¹ at around 14.2 cm⁻¹ kbar⁻¹, and which increases in intensity at the expense of the CH₂ twist, a result of decreased coupling between these modes. The antisymmetric CH₂ twist was not observed in any of IR or Raman spectra reported.

(iv) Pt-Cl Stretches

The symmetric and antisymmetric $\nu(\text{Pt-Cl}_2)$ modes at 336 and 330 cm⁻¹, respectively, were virtually coincident in the Raman spectrum. The antisymmetric mode was only visible as a shoulder on the broad symmetric band at 330 cm⁻¹. Both bands have similar pressure dependences and do not separate with pressure. Previous pressure work used to assign the symmetric and antisymmetric metal-halogen vibrational modes of solids, e.g., Pt(acac)Cl₂ and Pt(NBD)Cl₂,³⁰ has shown that the intensity of the symmetric mode decreases with respect to the antisymmetric mode. No such comparison could be

made here but the intensity of the trans-Cl mode increased in relation to the symmetric cis Pt-Cl mode. The pressure dependences of the $\nu(\text{Pt-Cl})$ internal modes, apart from the interatomic strain induced from pressure, are susceptible to the entire cell contents. Vibrational energies of solid salts show a marked dependence on the crystal structure and counter ions, for e.g., $\text{K}_2[\text{PtCl}_4]$.¹⁷ A study of the pressure dependences of a series of $\text{A}_2[\text{MCl}_6]$ complexes (where $\text{A} = \text{K}, \text{Cs}, \text{Rb}, \text{Ti}, \text{NH}_4$ and $\text{M} = \text{Pt}, \text{Sn}, \text{Te}$ and Pd) by Adams et al.³¹⁻³⁵ revealed that the γ_i , $d\nu/dp$ and the $d \ln \nu / dp$ values for the $\nu(\text{M-Cl})$ modes decreased in the order $\text{K} > \text{Rb} > \text{Cs}$ for a series of compounds with the same complex anion. Thus, the compressibility of the compounds are made up of contributions from both ions. The compressibility of the cation increases in the order $\text{K} > \text{Rb} > \text{Cs}$ as a larger amount of stress is needed to compress the shell.

There have been many reports on square-planar Pt(II) complexes in connection with the trans effect and the trans Pt-Cl bond distances.³⁶ The trans effect, as derived from kinetic data, suggests that ethylene is one of the most strongly trans activating ligands known,³⁷ and there is some evidence for a trans ligand influence leading to a weakening of the trans Cl bond. From X-ray³⁸ and neutron diffraction data,¹⁸ the Pt-trans Cl bond is slightly longer (ca. 0.04 \AA) than the average of the Pt-cis Cl bonds. However, the crystal packing and K^+ -Cl interactions can appreciably affect bond length,³⁹ and the individual Pt-Cl distances may be influenced by the pattern of $\text{K}^+ \dots \text{Cl}$ interactions in the unit cell. The trans Cl is in a unique position within the potassium cavity having four interactions with the K^+ cation versus one interaction with the cis Cl atom. The vibrational stretching frequency is also lower than that for the both Pt-cis Cl mode. However, the present concensus is that the trans influence may play a secondary role to the trans effect.³⁶ This may certainly be the case as the pressure dependences of both the cis and trans Pt-Cl stretches are virtually equal, although, according to Zallen,⁴⁰ pressure is expected to decrease the difference between the various force constants. The

Pt-trans Cl bond (force constant $\sim 1.78 \text{ mdyn } \text{\AA}^{-1}$) should be strengthened since its force constant is smaller than the Pt-cis Cl are ($\sim 2.2 \text{ mdyn } \text{\AA}^{-1}$).

(V) Skeletal Deformations

These modes have been assigned^{2,3} below 220 cm^{-1} . They share the same symmetry as the other modes and, therefore, are coupled. Two bands were observed in the Raman spectrum at 213 and 182 cm^{-1} with the former having a very large dv/dp value, $0.72 \text{ kbar}^{-1}\text{cm}^{-1}$, compared to the other values of the other vibrational modes. Although the exact composition of these bands is presently unclear, their differing behaviour with increasing pressure suggests that at least one of the two coupled modes which contribute to each band is substantially different. So far, the band at 213 cm^{-1} has been associated with a Pt-cis Cl_2 and $\text{Cl}_t\text{-Pt-C}_2\text{H}_4$ coupled bending mode.² Goggin and Mink¹⁷ have reported that the vibrational frequencies in $\text{K}_2[\text{PtCl}_4]$ are lower in solution than in the solid, but the effects are more pronounced for the Pt- Cl_2 bending modes than the stretching modes. Two contributing factors have been suggested to explain this effect: (1) Coupling of the bending modes to lattice modes and (2) the potassium cation interaction with the Pt- Cl_2 bonds. A similar pressure sensitivity was observed by Adams et al.³¹⁻³⁵ for the M- Cl_2 bending modes in the $\text{A}_2[\text{MCl}_6]$ complexes, where $\text{A} = \text{K}, \text{Rb}, \text{Cs}$ and $\text{M} = \text{Pt}, \text{Pd}$, etc. Apparently, this situation is caused by the K^+ ion compression forcing the neighbouring Cl ions apart on each C_3 face, resulting in a decrease in bond angle and an increase in strain and energy in the Pt- Cl_2 bending modes. Bending modes can also be dependent on the molecular geometry, as was observed by Wong⁴¹ for the N-Zn-N bending modes of $\text{Zn}(\text{CNPy})_2\text{Cl}$. As the two CNPy ligands approach each other upon compression, an increase in the repulsive force constant led to an increase in the energy of the bending mode. Apart from the lattice compression on the K^+ ions, a similar molecular geometrical deformation could be an additional factor in the increased

pressure dependence of the coupled Cl-Pt-C₂H₄ bending mode. The perpendicular orientation of the ethylene was attributed mainly to steric hindrance by the PtCl₃ moiety,⁴² so a decrease in this angle would be expected to increase the repulsive force constant between these two ligands and consequently cause an increase in energy in the bending mode. The other bending vibration at 182 cm⁻¹ displays a more normal pressure dependence, 0.39 kbar⁻¹ cm⁻¹. This band has been assigned to a coupled Cl₂-Pt-Cl and Pt-Cl₂ bending mode.²

The relative pressure sensitivities ($d \ln \nu / dp$) for the low-frequency stretching modes are significantly higher than the C-H stretching modes,⁴³ since the weaker bonds exhibit a greater relative susceptibility to compression. The C-H deformations and bending modes display smaller $d \ln \nu / dp$ values since their force constants depend less on interatomic distances. The nature of these vibrational modes also involves less volume change.

REFERENCES

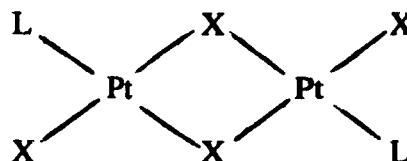
- (1) Rericha, R. *Coll. Czech. Chem. Comm.* **1975**, *40*, 2577.
- (2) Grogan, M. J.; Nakamoto, K. *J. Am. Chem. Soc.* **1966**, *88*, 5455.
- (3) Hiraishi, J. *Spectrochim. Acta.* **1967**, *25A*, 749.
- (4) Grogan, M. J.; Nakamoto, K. *J. Am. Chem. Soc.* **1968**, *90*, 918.
- (5) Jobic, H. *J. Mol. Spectrosc.* **1985**, *131*, 167.
- (6) Rericha, R. *Coll. Czech. Chem. Comm.* **1977**, *42*, 3518.
- (7) Powell, D. B.; Scott, J. G. V.; Sheppard, N. *Spectrochim. Acta.* **1972**, *28*, 327.
- (8) Hubert, J.; Konic, P. C.; Rochord, F. D.; Theophanides, T. *Can. J. Chem.* **1972**, *50*, 1596.
- (9) Andrews, D. C.; Davidson, G.; Duce, D. A. *J. Organomet. Chem.* **1975**, *101*, 113.
- (10) Pradilla-Sorzana, J.; Fackler, J. P. Jr. *J. Mol. Spectrosc.* **1967**, *22*, 80.
- (11) Mink, J.; Pápui, I.; Gái, M.; Goggin, P. L. *Pure Appl. Chem.* **1989**, *61*, 973.
- (12) Chatt, J.; Duncanson, L. A. *J. Chem. Soc.* **1953**, 2939.
- (13) Mingos, D. M. *Comprehensive Organomet. Chem.* **1982**, Vol. 3, 614.
- (14) Brundle, C. R.; Brown, D. B. *Spectrochim. Acta* **1971**, *27*, 2491.
- (15) Hartley, F. R. *Chemistry of Platinum and Palladium*; Applied Science Publishers: New York: **1973**.
- (16) Messter, M. A.; Stufkens, D. J.; Vrieze, K. *Inorg. chim. Acta* **1977**, *21*, 251.
- (17) Mink, J.; Gal, M.; Goggin, P. L.; Spencor, J. L. *J. Mol. Struct.* **1986**, *142*, 467.
- (18) Love, R. A.; Koetzle, T. E.; Williams, G. J. B.; Andrews, L. C.; Bau, R. *Inorg. Chem.* **1975**, *14*, 11, 2653.
- (19) Ferraro, J. R. *Vibrational Spectroscopy at High External Pressures*, Academic Press: New York **1984**.
- (20) Nakamoto, K.; Udovich, C.; Ferraro, J. R.; Quattrochi, A. *Appl. Spectrosc.* **1970**, *24*, *6*, 606.

- (21) Huang, Y.; Butler, I. S.; Gilson, F. R.; Lafleur, D. *Inorg. Chem.* **1991**, 30, 117.
- (22) Ferraro, J. C. *J. Chem. Phys.* **1969**, 53, 117.
- (23) Adam, D. M.; Ekejibuba, I. O. C. *J. Chem. Phys.* **1982**, 77, 4793.
- (24) Coffey, J. L.; Drickamer, H.G.; Park, J. T.; Roginski, R. T.; Shapley, J. R. *J. Phys. Chem.* **1990**, 94, 1981.
- (25) Ley, W. W.; Drickamer, H.G. *J. Chem. Phys.* **1989**, 93, 7276.
- (26) Ley, W. W.; Drickamer, H.G. *J. Chem. Phys.* **1989**, 93, 7257.
- (27) Huang, Y.; Butler, I. S.; Gilson, D.F.R. *Inorg. Chem.* **1992**, 31, 303.
- (28) Huang, Y.; Butler, I. S.; Gilson, D.F.R. *Inorg. Chem.* **1991**, 30, 1098.
- (29) Huang, Y.; Butler, I. S.; Gilson, D.F.R. *Spectrochim. Acta.* **1991**, 47A, 909.
- (30) Clarence, P.; Nakamoto, K.; Ferraro, J. R. *Inorg. Chem.* **1967**, 6, 2194.
- (31) Adams, D. M.; Berg, A. D.; Williams, A. D. *J. Chem. Phys.* **1981**, 5, 2800.
- (32) Adams, D. M.; Findlay, J. D.; Coles, M. C.; Payne, S. J. *J. Chem. Soc., Dalton Trans.* **1976**, 371.
- (33) Adams, D. M.; Payne, S. J. *J. Chem. Soc., Dalton Trans.* **1975**, 215.
- (34) Adams, D. M.; Ekejibuba, I. O. C. *J. Chem. Phys.* **1982**, 77, 4793.
- (35) Adams, D. M.; Payne, S. J. *J. Chem. Soc., Dalton Trans.* **1974**, 407.
- (36) Cotton, F. A.; Wilkenson, G. *Advanced Inorganic Chemistry*; Wiley Interscience: New York, 1980.
- (37) Appleton, T. G.; Clark, H. C.; Manzer, L. E. *Coord. Chem. Rev.* **1973**, 10, 335.
- (38) Jarvis, J. A.; Kilborn, B. T.; Osbourne, P. G. *Acta Cryst. Sect B* . **1971**, 27, 366.
- (39) Pratt, J. M.; Thorp, R. G. *Advan. Inorg. Chem. Radiochem.* **1969**, 12, 375.
- (40) Zallen, R.; Slade, M. L. *Phys. Rev. B: Conds. Matter* **1978**, B18, 5775.
- (41) Wong, P. T. T. *J. Chem. Phys.* **1983**, 78, 8.
- (42) Kuehn, G.; Taube, H. *J. Am. Chem. Soc.* **1976**, 98, 689.
- (43) Zallen, R. *Phys. Rev. B: Solid State* , **1974**, B9, 4485.

CHAPTER 5
ZEISE'S DIMER $[Pt(\eta^2-C_2H_4)Cl_2]_2$

5.1 Introduction

The structure of complexes of the general formula $[Pt(\eta^2\text{-olefin})X_2]_2$ is postulated to be trans-planar,^{1,2} with bridging halogens, as shown below:



where L=olefin and X=halogen. Such a structure has been established by single-crystal X-ray diffraction for the isomorphous palladium analogue of Zeise's dimer $[Pd(\eta^2-C_2H_4)Cl_2]_2$.³ Although the crystallographic space group and the exact positions of the two ethylene carbon atoms were not determined, the trans conformation was substantiated. However, owing to the lack of crystallographic data on complexes of the type $[Pt(\eta^2\text{-olefin})_2X_2]_2$, IR spectroscopy has been used as a source of structural information, especially in the far-IR region, where Pt-Cl vibrations are observed. Grogan and Nakamoto⁴ have studied the IR spectra of Zeise's dimer, the palladium analogue, and their deuterated analogues. The resemblance of vibrational frequencies in Zeise's salt and the dimer indicate that the electronic structure of these coordinated ethylenes are similar. Thus, as in the monomer complex, the C=C mode is coupled to a CH₂ deformation. These modes and the C-H twist mode show appreciable shifts on coordination from the free ethylene.⁴⁻⁶ However, the low-frequency IR region was used to differentiate between the monomer and dimer complexes. The authors assigned three bands in the far-IR to the Pt-Cl stretching vibrations. The Pt-Cl (terminal) mode absorbs in the 365-340

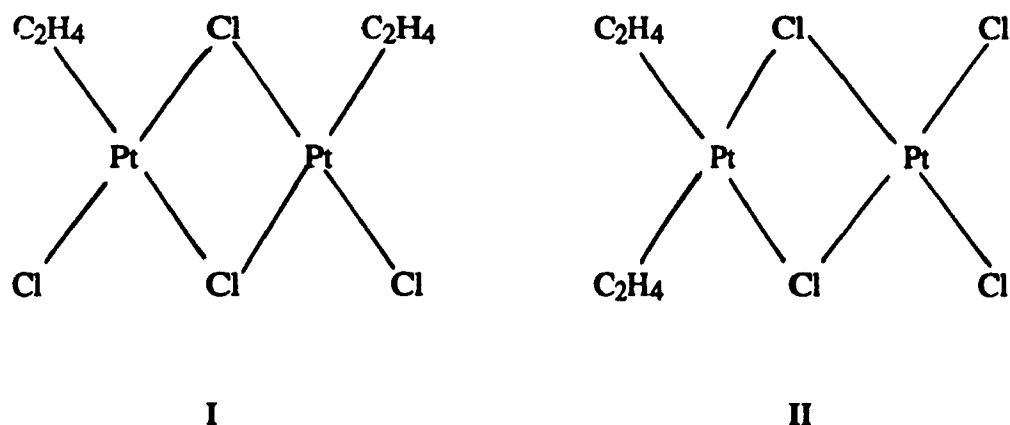
cm^{-1} region; only one band is expected since the terminal Pt-Cl bonds are equivalent with respect to the C_2 axis. The two Pt-Cl (bridging) stretching bands appear in the 325-300 and 295-270 cm^{-1} regions. The authors postulated that these assignments provided strong support for the centrosymmetric C_{2h} trans-planar model. In fact, the vibrational assignments proposed for Zeise's dimer and other similar $[\text{MX}_2\text{L}]_2$ complexes have been interpreted in terms of a trans halogen-bridged structure with C_{2h} point symmetry.^{7,8}

The IR vibrational bands observed under pressure in this thesis work are listed in Table 5.1.1 together with the calculated $d\nu/dp$ and $d \ln\nu/dp$ values. As in the case of Zeise's salt, the assignments are those given previously by Grogan and Nakamoto⁴ and Hiraishi.⁵ The wavenumber versus pressure plots are shown in Figure 5.1.1 and 5.1.2. The absence of any breaks in the slopes of the plots indicate that there were no pressure-induced phase changes throughout the pressure range investigated. All attempts to record the micro-Raman spectra failed. In addition to an intense fluorescence background, the sample burned rapidly under the 647.1 nm (red) Kr^+ ion laser excitation. At very low power, the peaks proved to be too weak to be detected and extended data accumulation only resulted in sample decomposition, due to the long laser exposure times necessary. The corresponding IR peaks were quite intense, but absorption due to the diamonds of the DAC completely masked the far-IR region.

Although all bands of the dimer in the infrared spectrum are coincident with Zeise's salt, the bands appear as doublets. The low-frequency Raman and IR spectra at ambient pressure are shown in Figures 5.1.3 and 5.1.4, respectively. There are a number of possibilities which can explain the doublets; however, the following factors have been excluded. Solid-state effects are unlikely since the solution far-IR displays the same doublet effect. The chlorine-isotope ($^{35}\text{Cl}/^{37}\text{Cl}$) effects are also unlikely since the band doubling is not observed in trans- PtCl_2L_2 compounds.⁸ The IR spectra of a number of complexes of the type PtCl_4L_2 ,⁷ showed the same multiplicity. This observation excludes the possible presence of more than one isomer, since it would imply the isomer

distribution is independent of the nature of the uncharged ligand. The same argument applies to the existence of the monomer. The possibilities that remain include a deviation from planarity in the four membered bridging ring where the resulting loss of symmetry would double the number of vibrational modes. This distortion is known to exist in $\text{Rh}_2\text{Cl}_2(\text{L})_4$,^{10,11} where $\text{L} = \text{CO}$ and C_2H_4 . A disymmetric ethylene orientation can also exist, as in $\text{Pt}(\text{dipentene})\text{Cl}_2$ ¹² which has one ethylene perpendicular to the PtCl_2 plane and the other is distorted to 62.1° . Disymmetric olefins are the result of a combination of steric, electronic, and crystal packing forces.¹³

The other isomers in addition to the trans isomer are shown below,



The cis isomer II is uncommon for the strong trans influencing C_2H_4 ligands.¹⁴ The gem-cis isomer I, point group C_{2v} , has been characterised by X-ray powder diffraction and far-IR, where it shows two intense trans Pt-Cl stretching bands.⁹ The doublet pattern confirms the C_{2v} symmetry. However, this isomer is only stable under an ethylene atmosphere. In conclusion, in view of the mentioned literature reports and the similarity of the far-IR and low-frequency Raman spectra to that assigned to the trans conformation,⁴ the peak doubling observed is most likely due to either a non-planar Pt- Cl_2 bridge or to a distorted disymmetric ethylene structure.

5.2 High Pressure Effects

The higher frequency components of the more clearly resolved doublets showed higher pressure dependences than did the lower frequency components. The application of pressure increased the intermolecular interactions and, therefore, led to the large pressure dependences of these particular peaks. With the exception of the C-H stretching modes, the resulting variations in pressure sensitivity and considerable bandwidth broadening of the vibrational modes indicate a difference in the compressibility between the monomer and dimer. The observed band broadening could be the result of a number of factors. As well as uneven pressure in the DAC, correlation coupling could also contribute to the broadening. At 2 cm^{-1} resolution, however, no splitting could be resolved. The C-H stretching modes for the dimer exhibited similar pressure dependences to those in Zeise's salt. The most noticeable differences in $d\nu/dp$ values between the two complexes were in the $\nu(\text{Pt-C}_2\text{H}_4)$ and the $\nu(\text{C}=\text{C})$ regions.

(i) Pt-C₂H₄ Stretch

The Pt-C₂H₄ antisymmetric stretch was observed at ambient pressure as a intense band at 490 cm^{-1} with a shoulder at 480 cm^{-1} . Between 10.2 and 12.4 kbar, this shoulder gained intensity and developed into a distinct peak, which continued to gain intensity until it eventually became much more intense than the original band. Because of the significant overlap of these bands, the errors in the measured peak position are large and so the resulting $d\nu/dp$ values are, at best, only estimates. It can be concluded, however, that the pressure dependences of the Pt-C₂H₄ stretching modes (0.19 and $0.41\text{ cm}^{-1}\text{ kbar}^{-1}$) are much less than in the monomer ($0.78\text{ cm}^{-1}\text{ kbar}^{-1}$). The only normal coordinate analyses performed for the coordinated ethylene in Zeise's dimer and its deuterio analog $[\text{Pt}(\text{C}_2\text{D}_4)\text{Cl}_2]_2$ were reported by Grogan and Nakamoto.⁴

Table 5.1.1 Pressure dependences of the Infrared Bands of Zeise's dimer.

ν (cm^{-1})	$d\nu/dp$ ($\text{cm}^{-1} \text{kbar}^{-1}$)	$d\ln\nu/dp$ ($\text{kbar}^{-1} \times 10^2$)	Assignments
490mw	0.19	0.038	Pt -C ₂ asym str. ^a
shoulder	0.41	0.085	
721mw	0.43	0.059	CH ₂ twist ^b
725mw	0.72	0.0099	
814w	0.14	0.017	CH ₂ rock
817w	0.26	0.031	
1020vs	0.00	0.0019	CH ₂ wag
1026vs	0.79	0.076	
1030vs	0.03	0.0029	
1179mw	0.33	0.027	CH ₂ rock
1234w	0.27	0.021	C=C str. ^a
1239mw	0.48	0.038	CH ₂ rock ^b
1413s	-0.13	-0.0092	CH ₂ sciss. + C=C str. ^b CH ₂ sciss. ^a
1427vs	0.05	0.0035	
1507w	0.32	0.021	C=C str + CH ₂ scicc. ^b CH ₂ sciss. ^a
1514w	0.23	0.015	
2981w	0.62	0.020	CH str.
3009w	0.46	0.015	
3071vw	0.68	0.022	
3084vw	0.68	0.021	
3096w	0.68	0.022	

^a From Grogan and Nakamoto ref.4. ^b From Hiraishi ref.5.

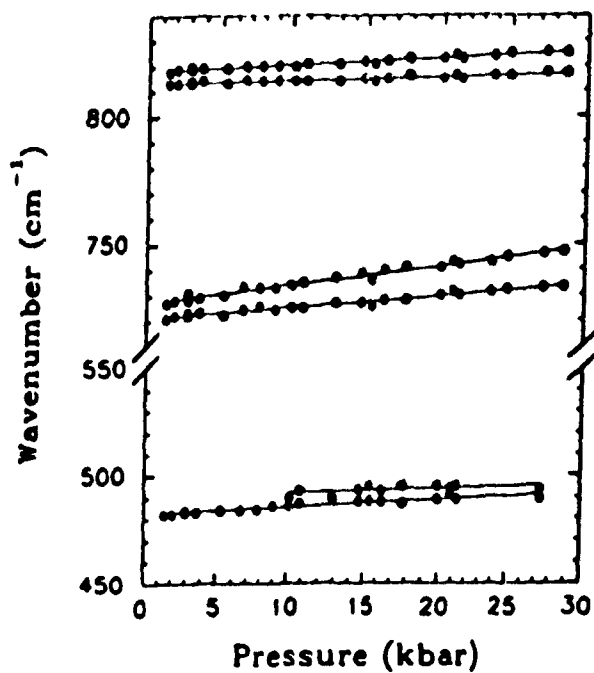


Figure 5.1.1 Pressure dependences of the IR peaks of Zeise's dimer (850-450 cm^{-1})

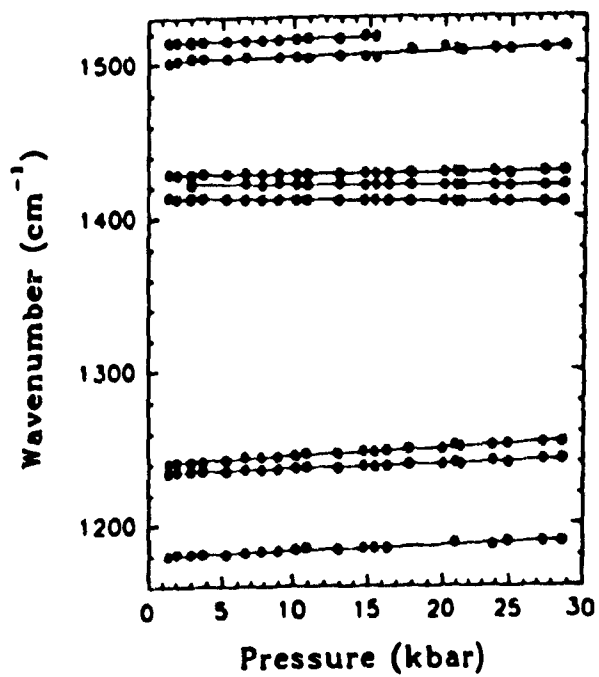


Figure 5.1.2 Pressure dependences of the IR peaks of Zeise's dimer (1520-1160 cm^{-1}).

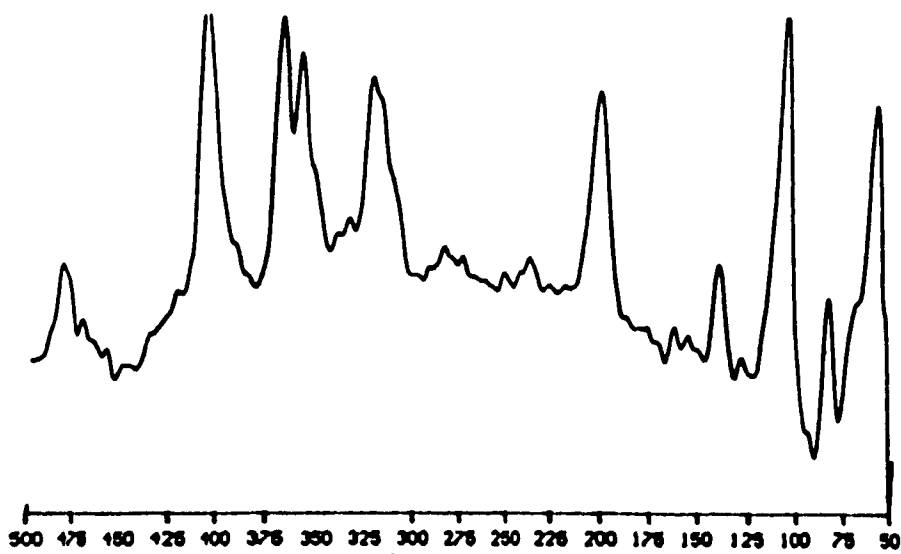


Figure 5.1.3 Raman spectra of Zeise's dimer at ambient pressure.

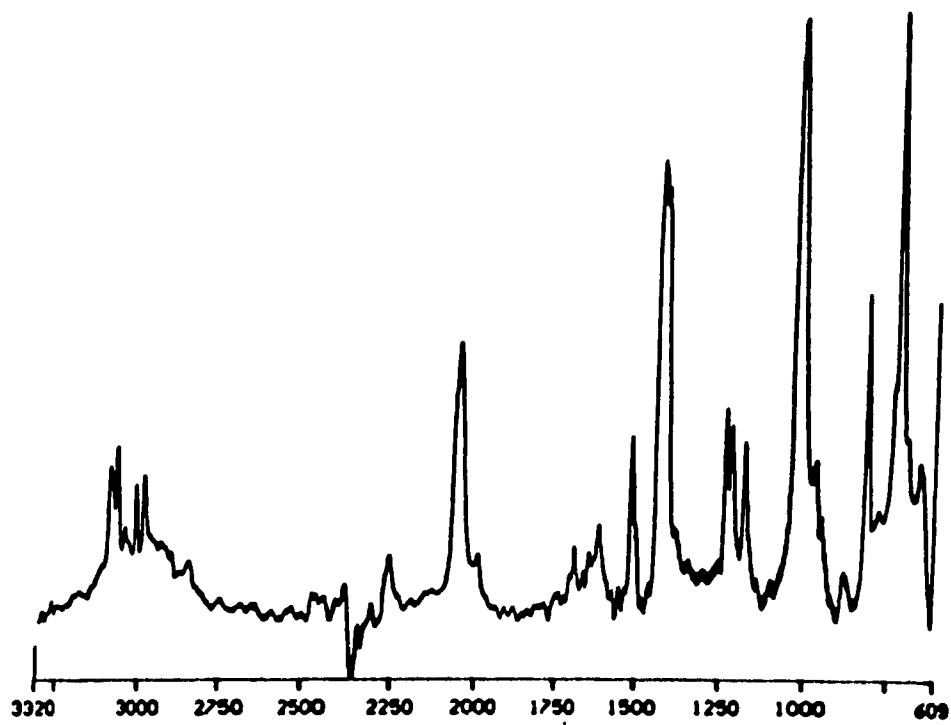


Figure 5.1.4 IR spectra of Zeise's dimer at ambient pressure

band at 406 cm^{-1} to the $\nu(\text{Pt-C}_2\text{H}_4)$ stretch mode, in both the monomer and dimer. The associated force constant, based on the same model as in Zeise's salt, was similar (2.23 mydnes/\AA) to that of the monomer (2.25 mydnes/\AA). This $\nu_s(\text{Pt-C}_2\text{H}_4)$ mode was not observed in the pressure IR study because the peak was buried beneath the strong diamond fluorescence. If the force constant for the observed $\nu_a(\text{Pt-C}_2\text{H}_4)$ mode in the monomer remains unchanged in the dimer, a similar pressure dependence would be expected. This was not the case. The bonding model used in these analyses has been criticized,¹⁵ and no definite comparison can be made between the Pt-ethylene bond strengths in the monomer and dimer on the basis of the available information.

(ii) C=C Stretch

The $\nu(\text{C}=\text{C})$ modes of Zeise's dimer are all observed as doublets, $1234/1239$, $1413/1427$ and $1502/1514\text{ cm}^{-1}$. The ethylene stretch is apparently coupled to a CH_2 deformation to the same extent as in Zeise's salt, since the frequency shifts upon coordination and with deuteration are similar.⁴ Unlike Zeise's salt, however, these modes increased in intensity with pressure, possibly the result of increased coupling. The bands in the 1200 and 1500 cm^{-1} regions broadened significantly, as in the monomer, while the 1413 cm^{-1} peak remained unchanged. The $1234/1239\text{ cm}^{-1}$ doublet was separated further from the calibrant peak than in Zeise's salt and these peaks displayed definite positive pressure dependences. The average of the $d\nu/dp$ and $d\ln\nu/dp$ values for this mode are the same as those for the monomer ($0.37\text{ cm}^{-1}\text{ kbar}^{-1}$ and $0.27\text{ kbar}^{-1}\times 10^2$ respectively). The weak $\nu(\text{C}=\text{C})$ mode located at $\sim 1500\text{ cm}^{-1}$, which was not observed for Zeise's salt under pressure, gave a clear absorbance in the dimer. The shoulder on the low-energy side became more defined at around 1.5 kbar . The relative intensity of these modes shifted from the higher- to the lower-frequency component with increasing pressure. Such

relative intensity changes are usually indicative of a Fermi resonance.^{17,18} With this in mind, a Sherman and Lewis analysis was attempted,¹⁹ but the resulting curves did not show the expected second-order curve fit to the calculated and observed peaks.²⁰ The near overlap of the broad band at 1427 cm^{-1} made measurement of the peak position difficult, even with spectral smoothing.

All bands in the $\nu(\text{C}=\text{C})$ stretch regions displayed positive pressure dependences with the exception of the 1413 cm^{-1} band, which had a negative $d\nu/dp$ value ($-0.13\text{ cm}^{-1}\text{ kbar}^{-1}$) analogous to that of the 1418 cm^{-1} band ($-0.08\text{ cm}^{-1}\text{ kbar}^{-1}$) in Zeise's salt. The broader band at 1427 cm^{-1} was virtually pressure insensitive ($0.05\text{ cm}^{-1}\text{ kbar}^{-1}$). Again, in an extension of Adams and Ekejiuba's theory,²¹ these pressure dependences suggest that the Pt-olefin π -backbonding was increased with increasing pressure. The lower frequency mode had the more negative pressure dependence and apparently reflected that this mode has a higher component of π backbonding. An important factor which may contribute to the different pressure sensitivity of the $\nu(\text{Pt}-\text{C}_2\text{H}_4)$ and $\nu(\text{C}=\text{C})$ stretches from those in the monomer is the absence of the K^+ counterion in the lattice. Since the compressibility of Zeise's salt arises from contributions from both types of ion, the dimer would be expected to display a different compressibility to that from the monomer. However, without an X-ray diffraction structure, the contribution from any changes in the bond lengths and the packing arrangement, remains unknown.

(iii) CH_2 Deformations

The CH_2 deformations showed more broadening and larger separations with increasing pressure than did the other vibrational modes. The CH_2 twist doublet at $721/725\text{ cm}^{-1}$ displayed a more positive pressure dependence (0.43 and $0.73\text{ cm}^{-1}\text{ kbar}^{-1}$) than the other CH_2 deformations. The same effect was observed in Zeise's salt. The three CH_2 wagging modes in the 1000 cm^{-1} region displayed more diverse behaviour.

The du/dp values differ considerably from each other and from those of the monomer. The peak intensities altered significantly with increasing pressure and it was difficult to measure the peak positions accurately, even after spectral smoothing. The single CH_2 rocking mode at 1179 cm^{-1} showed a shoulder on the low-energy side of the peak. This was the only mode in which the doublet was not resolved with pressure, presumably because both peaks have similar pressure dependences.

REFERENCES

- (1) Belluco, U. *Organometallic and Coordination Chemistry of Platinum*; Academic Press: 1974.
- (2) Hartley, F. R. *Chemistry of Platinum and Palladium*; Applied Science Publishers: 1973.
- (3) Dempsey, J. N.; Baenziger, N. C. *J. Am. Chem. Soc.* **1955**, *77*, 4984.
- (4) Grogan, M. J.; Nakamoto, K. *J. Am. Chem. Soc.* **1968**, *90*, 918.
- (5) Hiraishi, J. *Spectrochim. Acta* **1967**, *25A*, 749.
- (6) Jobic, H. *J. Mol. Spectrosc.* **1985**, *131*, 167.
- (7) Adams, D. M.; Chandler, P. J. *J. Chem. Soc. (A)* **1969**, 590.
- (8) Goodfellow, R. J.; Goggin, P. L. *J. Chem. Soc. (A)* **1967**, 1898.
- (9) Pregaglia, G. F.; Conti, F.; Minasso, B. *J. Organomet. Chem.* **1973**, *47*, 165.
- (10) Dahl, L. F.; Martell, C.; Wrangler, D. L. *J. Am. Chem. Soc.* **1961**, *83*, 1761.
- (11) Klarderman, K.; Dahl, L. F. *J. Organomet. Chem.* **1965**, *3*, 43.
- (12) Baenziger, N. C.; Medrud, R. C.; Dodge, J. R. *Acta Cryst.* **1965**, *18*, 237.
- (13) Mason, R.; Robertson, C. G. *J. Chem. Soc. (A)* **1969**, 492.
- (14) Purtemheimer, W.; Durham, B. *Inorg. Chem.* **1974**, *12*, 3800.
- (15) Mink, J. *J. Mol. Struct.* **1988**, *173*, 253.
- (16) Ley, W. W.; Dricckamer, H. G. *J. Phys. Chem.* **1989**, *93*, 7262.
- (17) Wong, P. T. T.; Chagwedera, T. E.; Mantsch, H. H. *J. Chem. Phys.* **1987**, *87*, 4487.
- (18) Tartag, A.; Fabre, D. *J. Chem. Phys.* **1987**, *87*, 981.
- (19) Sherman, W. F.; Lewis, S. *Spectrochim. Acta* **1979**, *35A*, 613.
- (20) Calculated by Dr. D. F. R. Gilson.
- (21) Adams, D. M.; Kejiuba, I. O. E. *J. Chem. Phys.* **1982**, *77*, 4793.

CHAPTER 6

Dichloro (1,5-cyclooctadiene)platinum (II) : Pt(COD)Cl₂

6.1 Introduction

Dienes able to act as bidentate chelating ligands form especially stable transition-metal complexes. 1,5-Cyclooctadiene (COD) affords the most stable complexes of the type Pt(diene)X₂, where X=halogen and diene = dicyclopentadiene, dipentene hexa-1,5 diene, and 1,5-COD.¹ The relative stabilities of Pt(COD)X₂ complexes have been established from kinetic studies of diene displacement reactions.² These reactions depend on the nature of the trans ligand, X. For X=Cl, the trans influence is minimal and COD displacement is difficult. Proton-NMR studies have shown that the J(Pt¹⁹⁵-H) couplings are quite large (75-80 Hz) for weak trans influence ligands.³ Gas-phase electron diffraction shows that free 1,5-COD exists in its C₂ twist boat conformation. Moreover, the X-ray diffraction of Pt(COD)Cl₂,⁴ the palladium analogue, and most of the (1,5 COD) metal complexes,⁵ show that complexed 1,5-COD retains the C₂ conformation.

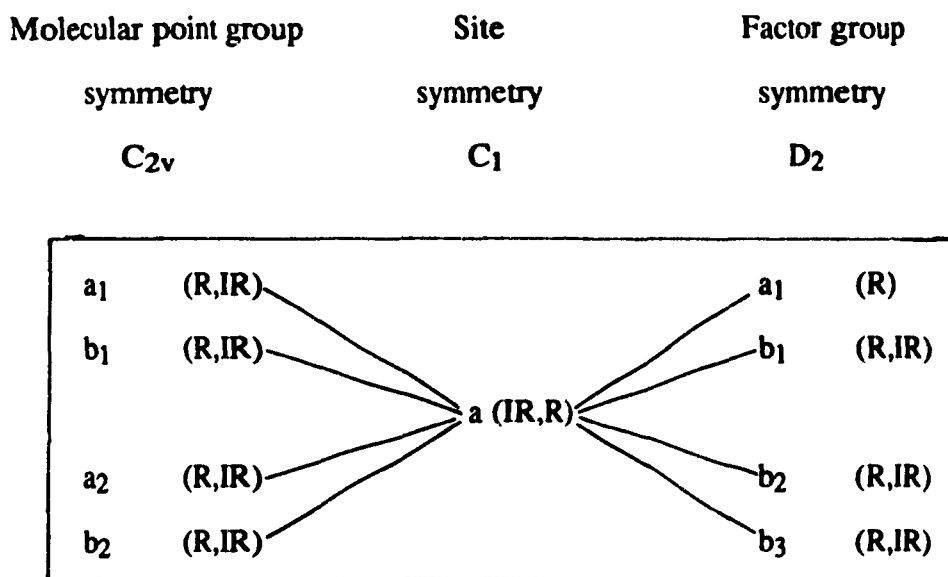
6.2 Factor group analysis

The Raman spectra of liquid and solid (-196°C) COD are very similar,^{6,7} as expected. The IR and Raman spectra of free COD have been tentatively assigned using the boat C_{2v} molecular point group.^{5,6} This 20-atom molecule has 54 fundamentals distributed as,

$$\Gamma_{\text{vib}} = 14a_1 + 14a_2 + 13b_1 + 13b_2$$

The factor group analysis for the C_{2v} molecular symmetry, C_1 site symmetry, and D_2 factor group symmetry [isomorphous with orthorhombic $P2_12_12_1$ (D_2) space group and $Z=4$] is shown in Figure 6.1.1. Correlation splitting is clearly expected in the crystal. The originally IR-inactive a_2 modes should become triplets (b_1, b_2, b_3) and quartets (a_1, b_1, b_2, b_3) in the IR and Raman spectra, respectively. The other vibrational modes of the free COD will have the same multiplicities in the crystal. Note that the factor group analysis based on C_2 molecular symmetry for the free COD molecule leads to the same spectral predictions for the COD crystal as for C_{2v} symmetry.

Figure 6.1.1 Factor Group Splitting of $Pt(COD)Cl_2$



6.3 High Pressure Effects

All bands broadened and decreased in intensity with pressure. Only a few of the vibrational peaks showed any splitting under pressure. One band, at 1016 cm^{-1} , formed a quartet in the Raman spectra under pressure (Figure 6.1.2). The IR spectrum at ambient pressure is given in Figure 6.1.3. The wavenumber versus frequency plots are shown in

Figures 6.1.4 and 6.1.5. for the IR (up to 26.8 kbar), and Figures 6.1.6 and 6.1.7 for the Raman spectra (up to 30.2 kbar). There are no breaks in the slopes and therefore no pressure-induced phase changes occurred throughout the pressure ranges investigated.

Two partial assignments have been attempted for the coordinated complex, mainly for the $\nu(\text{C}=\text{C})$ and $\nu(\text{Pt}-\text{COD})$ vibrational stretching modes.^{8,9} Both reports follow the work of Hiraishi¹⁰ and assigned two $\nu(\text{C}=\text{C})$ modes, as a result of the CH_2 deformation coupling, and two $\nu(\text{Pt}-\text{COD})$ modes, in accordance with the cyclopropane model. Wertz et al.^{9,11,12} have produced a number of vibrational assignments on metal-cyclic mono and diolefin complexes. The proposed assignments, together with the calculated $d\nu/dp$ and $d \ln\nu/dp$ values from the IR and Raman high pressure data, are listed in Table 6.1.1. The a_1 symmetric modes were assigned on the basis of their solution Raman polarisations while the $\nu(\text{Pt}-\text{Cl})$ modes were assigned by analogy with the bromo analogue. Owing to the complexity of the COD vibrational modes, bands that did not show a significant shift upon coordination of more than 1%, were left unassigned - these are most likely CH_2 modes.

From high-pressure studies performed on the highly strained cage compounds norbornadiene, norbornylene and norbornane,¹³ some spectral assignments were possible from their relative pressure dependences of certain bands. In general, the C-H stretch modes displayed larger and more varied pressure dependences in comparison to the ring C-C stretching modes, the C-H bond length being dependent on the angle strain. The C-H deformations had lower $d \ln\nu/dp$ values than the skeletal vibrations and the C-C stretching modes. In the COD complex, most of the pressure dependences of the vibrational bands below 2900 cm^{-1} lie within a narrow range, $0.2 - 0.38 \text{ cm}^{-1} \text{ kbar}^{-1}$ in the IR spectra, and 0.2 and $0.51 \text{ cm}^{-1} \text{ kbar}^{-1}$ in the Raman spectra. Unlike the highly strained cage compounds, COD is more flexible, and the compressibilities of different bonds with pressure show no significant differences. Therefore, no further assignments can be given. However, the C-C-C ring bending modes should show a relatively small pressure

Table 6.1.1 Pressure dependences of the Infrared and Raman peaks of $(\text{Pt}(\text{COD})\text{Cl}_2)$

INFRARED			RAMAN			Assignments
ν (cm^{-1})	$d\nu/dp$ ($\text{cm}^{-1} \text{ kbar}^{-1}$)	$d\nu/dp$ ($\text{kbar}^{-1} \times 10^2$)	ν (cm^{-1})	$d\nu/dp$ ($\text{cm}^{-1} \text{ kbar}^{-1}$)	$d\nu/dp$ ($\text{kbar}^{-1} \times 10^2$)	
			310s	0.41	0.13	} Pt-Cl str.
			338s	0.51	0.016	
			382m	0.40	0.010	
457w	0.34	0.074	456vs	0.45	0.098	} ν_s (Pt-C ₂ H ₄)
475m ^w	0.37	0.077	476s	0.31	0.065	
			512m	0.31	0.074	} ν_a (Pt-C ₂ H ₄)
582w	0.32	0.054	582m	0.33	0.053	
645w	0.26	0.037				
780w	0.35	0.044	782	0.44	0.056	ρ_r (C-H)
810m	0.33	0.040				a ₁
833w	0.35	0.042				
872w	0.35	0.040				ρ_r (C-H)
911w			906vs	0.39	0.042	ρ (C-C-C)
			980w	0.22	0.022	
1011s	0.16	0.015	1014w	0.09	0.008	
			1016mw	0.49	0.048	
1029w	0.30	0.029	1024w	1.00	0.098	a ₁
1075w	0.24	0.022				
1088w	0.38	0.034				a ₁
1180m	0.20	0.016				ρ_w (C-H)
1226w	0.22	0.017				a ₁
1242w	0.20	0.016	1244m	0.20	0.016	a ₁ ρ_w (C-H) + ν (C=C)
1340m	0.12	0.0089				
1402s	0.21	0.015				
1426m	-0.18	0.004				a ₁
1451m	0.06	0.0041				a ₁ δ (CH ₂)
1476s	0.23	0.015	1478m	0.21	0.013	
			1490m	0.30	0.020	
1499w	0.25	0.016	1500s	0.35	0.023	ν (C=C) + ρ_w (CH)

Table 6.1.1 (cont'd)

INFRARED			RAMAN			Assignments
ν (cm^{-1})	$d\nu/dp$ ($\text{cm}^{-1} \text{kbar}^{-1}$)	$d\ln\nu/dp$ ($\text{kbar}^{-1} \times 10^2$)	ν (cm^{-1})	$d\nu/dp$ ($\text{cm}^{-1} \text{kbar}^{-1}$)	$d\ln\nu/dp$ ($\text{kbar}^{-1} \times 10^2$)	
			2911w	1.35	0.046	C-H str.
			2933m	1.32	0.046	
			2920m	0.54	0.018	
2943s	0.73	0.024				
2962s	0.84	0.028	2967ms	0.49	0.016	
3009s	0.25	0.083	3010ms	0.37	0.012	
3023s	0.30	0.099	3022m	0.45	0.014	

dependence,¹⁴ since these are less dependent on the force constants. The small $d\nu/dp$ values for the bands at 1011 and 1340 cm^{-1} indicates that these bands can be tentatively assigned to these modes. In the following sections, the more important regions will be discussed, viz., $\nu(\text{C}=\text{C})$, $\nu(\text{Pt}-\text{COD})$, and the 2900-3000 cm^{-1} region.

(i) C=C Stretch

The C=C stretching modes in free COD have been assigned^{6,7} to the intense polarised bands at 1660 and 1266 cm^{-1} . The assignment of the $\nu(\text{C}=\text{C})$ bands in the complex was hampered by the overlap with the C-H bending fundamentals of the COD ligand. However, these modes have been assigned at 1500 and 1200 cm^{-1} , based on the strength of the polarised bands in these regions and also on the approximate frequency shifts from the free olefin (160 cm^{-1}), which are usually reported¹⁵ between 120-160 cm^{-1} . The $\nu(\text{C}=\text{C})$ stretch in other $[\text{Pt}(\text{olefin})\text{Cl}_2]$ complexes, where olefin= dipentene¹ and cyclopentene,¹² shifts over 200 cm^{-1} on coordination.

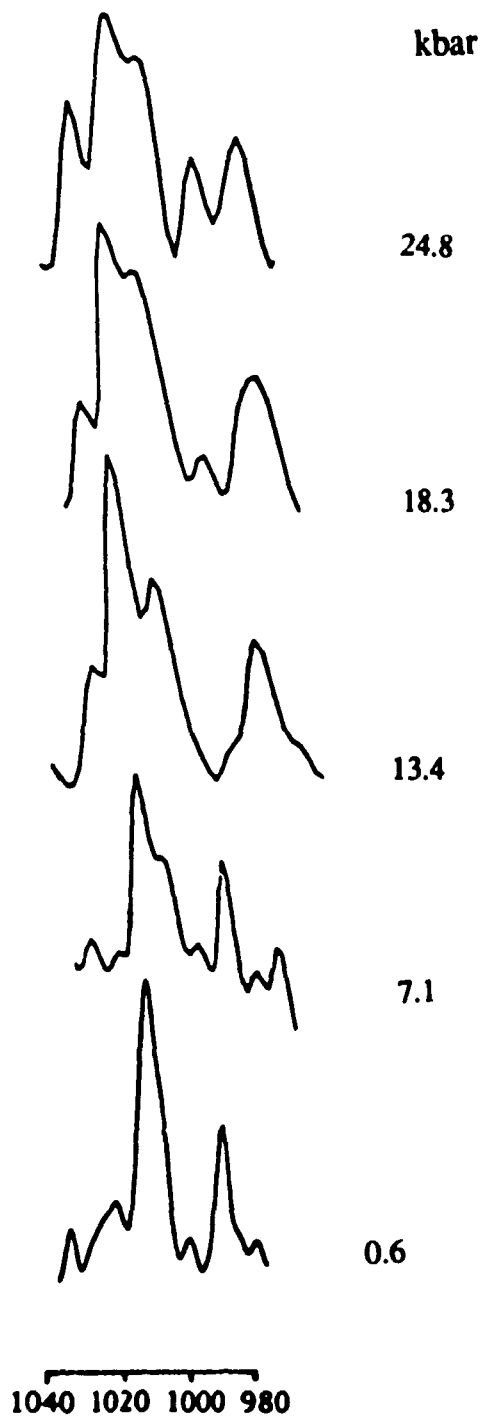


Figure 6.1.2 Raman spectra of the band at 1014 cm^{-1} at the indicated pressures upon compression.

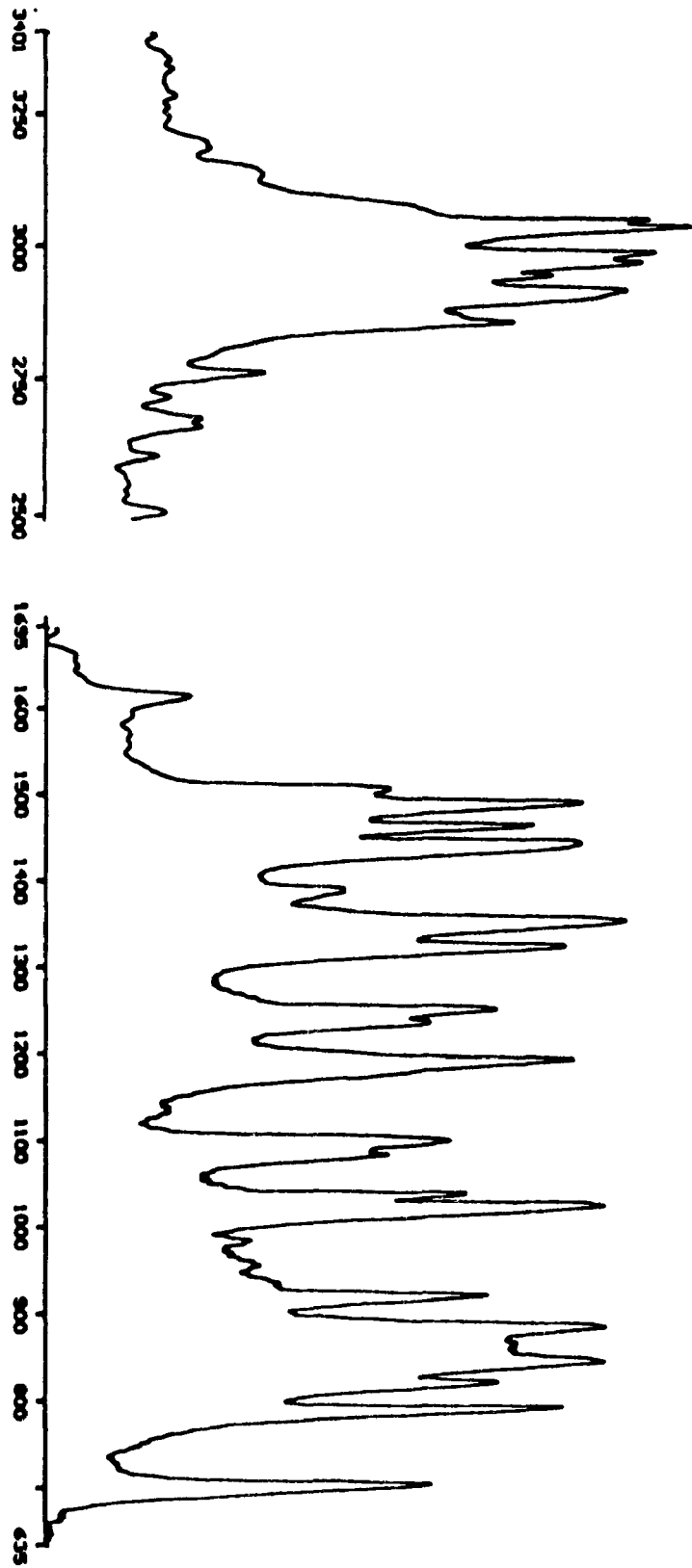


Figure 6.1.3 IR spectra of [Pt(COD)Cl₂] at ambient pressure.

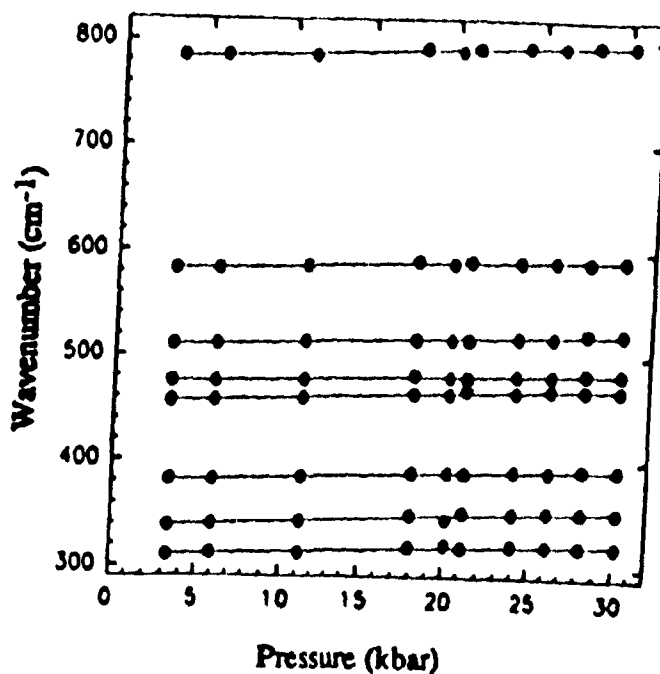


Figure 6.1.4 Pressure dependences of the IR peaks of $[\text{Pt}(\text{COD})\text{Cl}_2]$ (800-300 cm^{-1}).

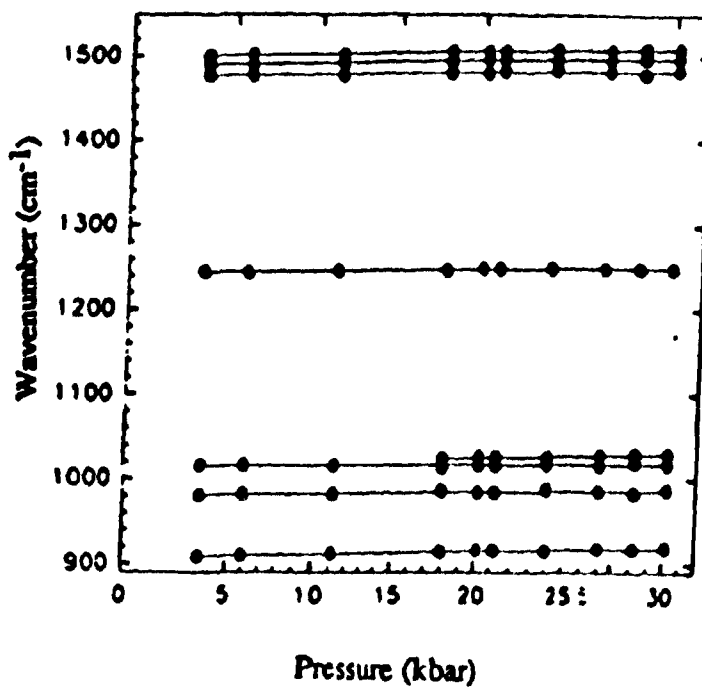


Figure 6.1.5 Pressure dependences of the IR peaks of $[\text{Pt}(\text{COD})\text{Cl}_2]$ (1540-900 cm^{-1}).

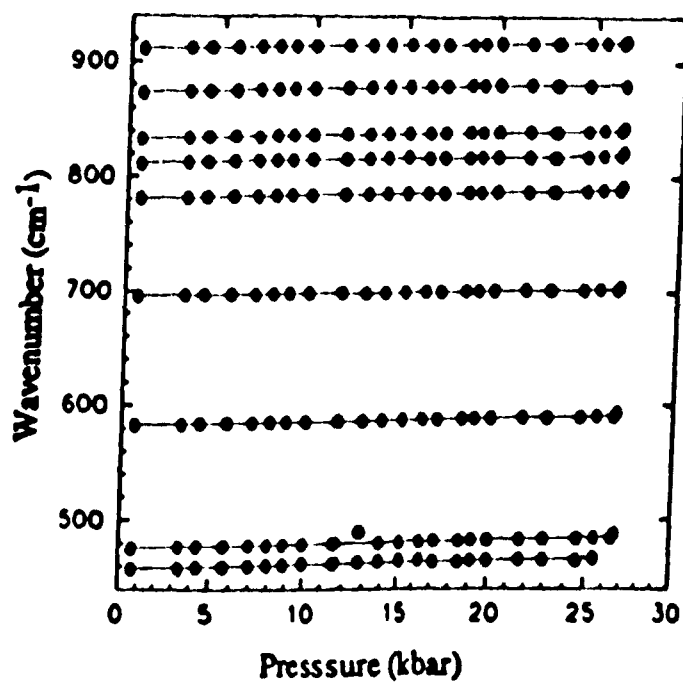


Figure 6.1.6 Pressure dependences of the Raman peaks of [Pt(COD)Cl₂] (920-460cm⁻¹).

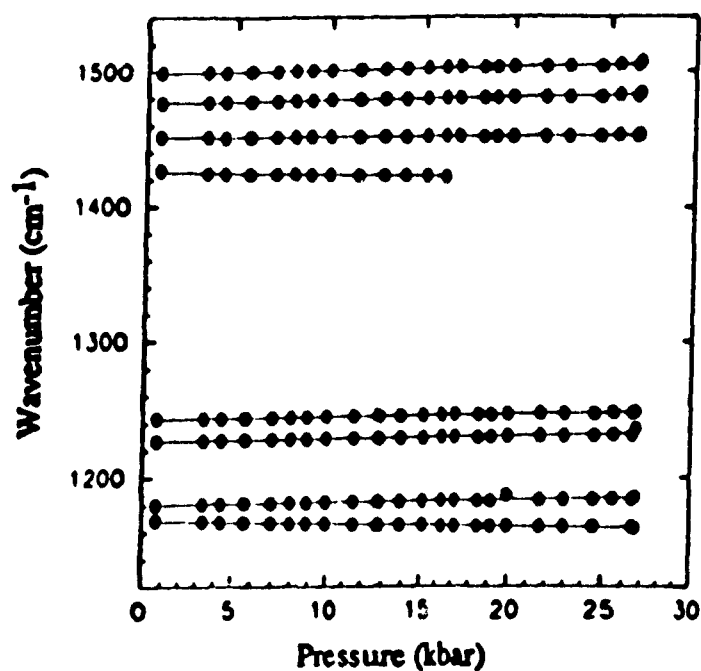


Figure 6.1.7 Pressure dependences of the Raman peaks of [Pt(COD)Cl₂] (1520-1120 cm⁻¹).

The dv/dp for the band at 1500 cm^{-1} in the IR spectra is within the narrow dv/dp range found for most of the modes, whereas the 1426 cm^{-1} band, which is strongly polarised, showed a negative dv/dp value ($-0.18\text{ cm}^{-1}\text{ kbar}^{-1}$). The same band collapsed in the Raman at high pressure and could not be measured. However, in the IR spectrum, this band was only measured up to $18.5\text{ cm}^{-1}\text{ kbar}^{-1}$, at which point the intense band originally located at 1402 cm^{-1} moved over this peak. The medium strong band at 1426 cm^{-1} also occurs in $\text{Pt}(\text{COD})\text{R}_2$ derivatives, where $\text{R} = \text{CH}_3$, *o*- and *p*- $\text{CH}_3\text{C}_6\text{H}_4$ and *1*- C_{10}H_7 , and was assigned to the C=C stretching mode.¹⁶ In conclusion, the 1426 cm^{-1} band in $\text{Pt}(\text{COD})\text{Cl}_2$ was reassigned to a $\nu(\text{C}=\text{C})$ stretch. The other $\nu(\text{C}=\text{C})$ band assigned at 1242 cm^{-1} , has the same dv/dp value ($0.20\text{ cm}^{-1}\text{ kbar}^{-1}$) in both the IR and Raman spectra, and this positive pressure dependence confirms the reported assignment,⁹ in that this $\nu(\text{C}=\text{C})$ is more strongly coupled to the CH_2 deformation.

(ii) (Pt-C₂H₄) Stretches

There are four Pt-olefin bands tentatively assigned⁹ in the $500\text{-}350\text{ cm}^{-1}$ region. Free COD has four twist/torsion vibrational modes in this region also, which could couple to the metal-olefin motions. In order to differentiate between the σ and π bonding components, Wertz^{9,11,12} described the motion of the carbons of the metal-olefin tilt mode as moving into and out of the π -electron density region. This particular mode moves up in frequency upon complexation, from 200 to $350\text{-}500\text{ cm}^{-1}$, and is described as the antisymmetric Pt-COD mode. Therefore, the symmetric and asymmetric modes are expected to behave differently, depending on the extent of metal-olefin π -bonding in different complexes. This theory should also apply in high pressure vibrational studies. From the dv/dp and $d \ln \nu/dp$ values determined for the $\nu(\text{Pt-olefin})$ modes, the values of the antisymmetric modes are lower than the symmetric modes. This behaviour is usually

attributed to the particular vibrational motion of an asymmetric mode, the direction being nearly opposite to that of the pressure. However, this pressure sensitivity could also be indicative of some contribution from a stronger π -bonding system

(iii) C-H Stretching Region

At ambient pressure, nine bands were observed in the 2800-3030 cm^{-1} region in the Raman spectrum. The bands broadened significantly with pressure and eventually produced six broad bands, with the intensity of the bands above 3000 cm^{-1} decreasing significantly more than the other modes. These high-energy bands displayed very different pressure dependences, the two lower frequency bands having much higher $d\nu/dp$ values, 1.35 and 1.32 $\text{cm}^{-1} \text{ kbar}^{-1}$. The wavenumber versus pressure plot is shown in Figure 6.1.8. This high-frequency region was unassigned, but the antisymmetric and symmetric C-H and methylene stretch bands are expected to be coupled in this region. However some possible assumptions can be made for their pressure behaviour, which will be discussed in the following section.

(iv) Discussion

The structural conformation of 1,5-COD plays a primary role in securing a more stable π -bonded coordinated complex. The X-ray diffraction studies of $\text{Pt}(\text{COD})\text{Cl}_2$ reported in the literature^{4,17} are somewhat questionable, as a number of discrepancies exist in the structural parameters, e.g., in the dihedral angle, the ethylene orientation and the approximate hydrogen positions and distances. Force field calculations have proven to be an important method of estimating the most stable conformation of cyclic ring structures. There have been numerous reports of ring structures calculated by molecular

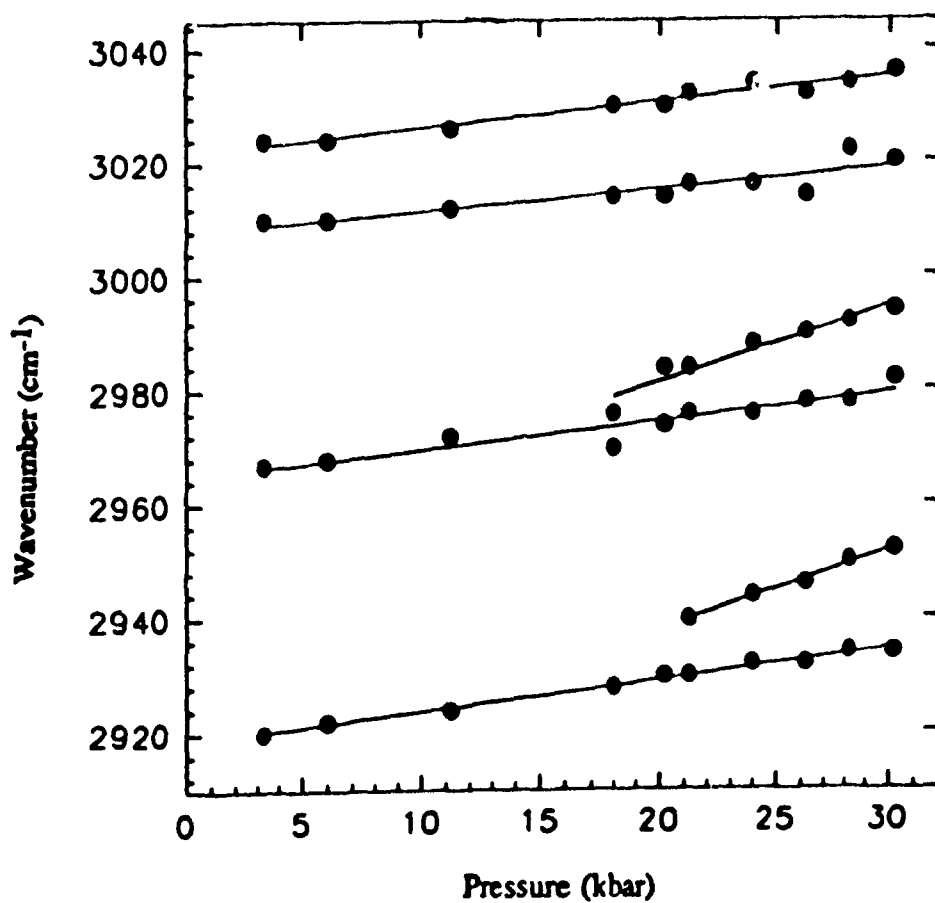


Figure 6.1.8 Pressure dependences of the Raman peaks in the C-H stretching region of $[\text{Pt}(\text{COD})\text{Cl}_2]$

mechanics and, in particular, those of square-planar medium-sized ring diene chelating complexes.⁵ The observed conformation of a coordinated diolefin can differ dramatically from that of the most stable form of the free ligand. In the case of 1,5-COD, the calculated free ligand conformation⁸ is very similar to that of the C₂ coordinated structure. Therefore the minimum energy conformation of the free diene changes relatively little on coordination.⁵ The twist boat is characterized by a low strain energy, 13.43 kcal mol⁻¹, yet appreciable angle (torsion) strain, the dihedral angle C-CH₂-CH₂-C being 52.5°. This strain originates from a trans-annular methylene H...H repulsion, the methylene hydrogens are staggered to avoid being eclipsed, as in the C_{2v} boat conformation. The calculated H...H distance is 1.99 Å, which is slightly longer than the minimal distance (1.7 Å) required by the Van der Waal's repulsion force. A molecular mechanics study was performed in this work¹⁹ for the COD twist boat and chair conformations, using Allinger's MM2 program and PC Model. Table 6.1.2 lists some of the parameters calculated. The former study minimised a twist boat conformation with a considerable low strain energy, 14.09 kcal mol⁻¹, and the transannular H...H distance is relatively long at 2.13 Å. The alternative PCModel, calculated a much smaller energy difference between the two conformations. The strain energy of the twist boat approaches that of the more rigid chair conformation, with only 0.51 kcal mol⁻¹ difference between them, the high torsion dihedral angle remains at 103°. The H...H distance at 1.98 Å and the C₂C₃C₄C₅ dihedral angle of 53° are similar to the values reported by Ermer.¹⁸ It is important to note that the MM2 parameters used for the non-bonded interactions involving hydrogens are too repulsive at short distances and have been revised²⁰ in MM3. The MM2 calculations have too strong an interaction between the trans-annular hydrogens, leading to a lower dihedral angle at C₂C₃C₄C₅. Therefore, from the above analysis, the 1,5-COD twist boat would appear to be quite flexible, in that the hydrogens can approach each other relatively closely. This flexibility could be an

important geometric factor which can contribute to the extent of overlap of the molecular orbitals involved in the metal-ligand bond.

Table 6.1.2

Parameters	MM2		PCModel	
	Boat	Chair	Boat	Chair
Total Energy (kcal mol ⁻¹)	15.73	16.99	17.54	18.03
Bend (kcal mol ⁻¹)	3.81	1.72	5.25	1.73
Strain Energy (kcal mol ⁻¹)	14.09	15.35	15.90	16.41
Dihedral Angle	41°	103°	53°	103°
r (H...H)	2.13 Å		1.98 Å	

There are two competing factors involved in the metal-ligand π -bond overlap. (1) The minimal energy C_2 conformation induces an increased torsion angle to minimize the eclipsed H...H repulsion and, at the same time, causes a slight non-planar deformation of the ethylene double bonds. This twist, known as the torque angle, is the rotation about the perpendicular C=C plane normal to the PtCl₂ plane, and would decrease the π -bond overlap. (2) The platinum d-orbitals require the parallel ethylene orientation, of the more strained C_2 boat conformation, for maximum π -bond overlap. The most stable conformation in the Pt(COD)Cl₂ complex requires an energy equilibrium between these two factors. There are a number of cases in cyclic metal complexes where the parallel geometry is already constrained. In Pt(NBD)Cl₂,¹¹ where NBD=norbornadiene, the free ligand is highly strained,²¹ the strain energy calculated at 33.59 kcal mol⁻¹. Upon coordination, a very stable complex is formed, with only minor conformational changes. The ethylene bonds are coplanar and maximise the π -bond overlap. Although the π bonds of the NBD complex are at an angle to the plane normal to the ethylene plane, the

ideal nonbonded distance between the ethylene bonds (2.88\AA), compensates to allow a strong metal-olefin overlap. The complexes $\text{Pd}(\text{diene})\text{Cl}_2$, where diene=1,4-COD and 1,5-cyclononadiene, coordinate in a more strained 'excited' form in so that the olefins can be rotated to the correct parallel orientation.⁵ The shift towards sp^3 hybridization at carbon upon coordination can allow strained olefins to bind more strongly to the metal than the unstrained olefins, as illustrated by the displacement of coordinated cis-cyclooctene by the more strained trans isomer in $\text{Cr}(\text{CO})_5(\text{cyclooctene})$.²²

A more recent low-temperature (110 K) X-ray diffraction study on $\text{Pt}(\text{COD})\text{Cl}_2$ reports an even larger distortion to C_s symmetry.¹⁷ The authenticity of this X-ray study is questionable, considering that all the thermal ellipsoids are unusually small and the Cartesian coordinates do not conform to the same conformational parameters reported. Ermer¹⁸ has described a twistboat/twistboat potential energy profile via a C_s intermediate conformation. This conformation is shown to have planar ethylene bonds and a calculated strain energy of $17.5 \text{ kcal mol}^{-1}$. This process is given as a possible explanation for an observed ^1H NMR coalescence at 105 K.

The high-pressure studies in this work will be used primarily to show the presence of π -backbonding, as in the previous chapters. However, the extent to which this is affected by a number of factors including the conformational differences discussed above and an additional possible contribution from crystal packing forces, will be considered.

The retention of the twist boat conformation may be indicated by the unusual behaviour of the C-H stretching modes under high pressure (Figure 6.1.7). The lower frequency modes at 2911 and 2933 cm^{-1} display very high pressure dependences. These modes can be tentatively assigned to the antisymmetric CH_2 modes. The symmetric stretch of the methylene trans-annular hydrogens would be expected to be very pressure insensitive, since the repulsion between them is strong enough to distort the boat C_{2v} conformation to the C_2 symmetry structure. Moreover, because the effect of pressure pushing these opposing hydrogens together would hinder the symmetric more so than the

antisymmetric stretches, the symmetric modes can therefore be assigned to the bands with lower $d\nu/dp$ values at 3010 and 3022 cm^{-1} . The ethylene hydrogens have a higher force constant but a shorter C-H bond distance and should display a high pressure sensitivity. Even though the force constant is higher, the percentage decrease in bond distance with pressure should be large. The IR bands at 2943 and 2967 cm^{-1} have $d\nu/dp$ values, 0.73 and 0.84 $\text{cm}^{-1} \text{kbar}^{-1}$, similar to the ethylene C-H symmetric modes in Zeise's salt and its dimer.

REFERENCES

- (1) Chatt, J.; Vallarino, L. M.; Venazi, L. M. *J. Chem. Soc.* **1957**, 2496.
- (2) Volger, C. H.; Grassbeek, M. M. P.; Hogeveen, H.; Vrieze, *Inorg. Chim. Acta* **1969**, 3, 145.
- (3) Clark, C. M.; Manzer, L. E. *J. Organomet. Chem.* **1973**, 59, 411.
- (4) Goel, A. B.; Goel, S.; Veer, D. V. D. *Inorg. Chim. Acta* **1982**, 65, L205.
- (5) Rettig, M. F.; Wing, R. M.; Wiger, G. R. *J. Am. Chem. Soc.* **1981**, 103, 2980.
- (6) Barna, G. C.; Butler, I. S. *J. Raman Spectrosc.* **1978**, 7, 168.
- (7) Mendra, P. J.; Powell, D. B. **1961**, 17, 913.
- (8) Powell, D. B.; Leedham, T. J. *Spectrochim. Acta* **1972**, 28, 337.
- (9) Wertz, D. W.; Moseley, M. A. *Inorg. Chem.* **1980**, 19, 705.
- (10) Hiraishi, J. *Spectrochim. Acta* **1967**, 25A, 749.
- (11) Wertz, D. W.; Moseley, M. A. *Spectrochim. Acta* **1980**, 36, 467.
- (12) Wertz, D. W.; Bocian, D. F.; Hazouri, M. J. *Spectrochim. Acta* **1973**, 29, 1439.
- (13) Kawai, N.; Ph.D Thesis, McGill University, Montreal, 1991.
- (14) Ferraro, J. R. *Vibrational Spectroscopy at High External Pressures*; Academic Press: 1984.
- (15) Hartley, F. R. *Comp. Organometal Chem.* **1982**, Vol. 6.
- (16) Kistner, C. R.; Hutchinson, J. H.; Doyle, J. R.; Storlie, J. C. *Inorg. Chem.* **1963**, 2, 1255.
- (17) Ashfaquzzam, S.; Stevens, E. D.; Cruz, S. G. *Inorg. Chem.* **1984**, 23, 3673.
- (18) Ermer, O. *J. Am. Chem. Soc.* **1976**, 98, 3964.
- (19) Calculated by Dr. D. F. Gilson.
- (20) Allinger, N. L.; Yub, Y. H.; Lii, J. H. *J. Am. Chem. Soc.* **1989**, 111, 8551.
- (21) Allinger, N. L.; Spague, J. L. *J. Am. Chem. Soc.* **1972**, 94, 5734.
- (22) Grevels, F. W.; Skibbe, V. *J. Chem. Soc., Chem. Commun.* **1984**, 6814.

CHAPTER 7
CONCLUSIONS

The high-pressure infrared and micro-Raman spectra of crystalline Zeise's salt, $K[Pt(\eta^2-C_2H_4)Cl_3]$, Zeise's dimer, $[Pt(\eta^2-C_2H_4)Cl_2]_2$ and dichloro(η^2 -cyclooctadiene)platinum(II), $Pt(COD)Cl_2$, have been studied to examine the π -backbonding interactions of the metal-olefin bonds under high external pressures. The effect of pressure on the $Pt-C_2H_4$ π bond is shown to be similar to that in other π -bonded systems such as $M-C=O$.¹⁻⁷ The $Pt-C_2H_4$ bond strengthens as the extent of the π -backbonding from the metal to the π^* -orbital in the C_2H_4 ligand increases with pressure. This pressure effect then shifts the $C=C$ stretching modes to lower wavenumbers. The resultant lengthening of the $C=C$ bonds is indicated by a negative or zero pressure dependence, dv/dp . The experimentally observed pressure dependences of the $\nu(C=C)$ modes are the net result of the crystal lattice compression and concomitant decreases in the intermolecular and interatomic distances. There is also appreciable coupling between the $\nu(C=C)$ stretching and $\delta(CH_2)$ deformation modes, and this is expected to contribute positively to the pressure sensitivity. In addition, in the COD complex and Zeise's dimer, the possible unequal distribution of π -backbonding in the two ethylene bonds may also be caused by unsymmetrically bonded ethylene bonds. Crystal packing forces and molecular conformational changes are known to distort the ideal perpendicular orientation of the ethylene bonds towards the metal d orbitals.⁸ In spite of a considerable amount of earlier work on Zeise's salt, there is still some controversy regarding the vibrational assignment of the spectra. The basic work of Hiraishi,⁹ and, partly that of Grogan and Nakamoto,¹⁰ has led to the generally accepted assignment, which was later used to assign the vibrational spectra of other π -bonded metal-olefin coordinated complexes. Table 7.1.1 summarises the dv/dp values observed for the IR bands

associated with the $\nu(\text{C}=\text{C})$ stretching modes. The flexibility of the olefinic ligands could be an important geometric factor which can contribute to the extent of the π -backbonding.

Table 7.1.1

Pt(η^2 -C ₂ H ₄)Cl ₃		[Pt(η^2 -C ₂ H ₄)Cl ₂] ₂		Pt(COD)Cl ₂	
ν (cm ⁻¹)	dν/dp (cm ⁻¹ kbar ⁻¹)	ν (cm ⁻¹)	dν/dp (cm ⁻¹ kbar ⁻¹)	ν (cm ⁻¹)	dν/dp (cm ⁻¹ kbar ⁻¹)
1252	0.37	1234	0.27	1242	0.20
		1239	0.48		
1418	-0.08	1413	-0.13	1426	-0.18
1515		1427	0.05	1499	0.25
		1514	0.23		

On the basis of previous work by Adams and Ekejiuba on metal-C=O systems,⁶ the negative dν/dp values of the $\nu(\text{C}=\text{C})$ stretching modes are indicative of a stronger π -backbonding effect with pressure. The $\nu(\text{C}=\text{C})$ stretching modes in the 1500 and 1200 cm⁻¹ regions have been previously assigned⁹ on the basis of the intense polarised bands in the solution Raman spectra and the observed frequency shifts from the free ethylene value upon coordination. In agreement with the most recent vibrational assignment on Zeise's salt,¹¹ the dν/dp values indicate that the polarised bands at ~1200, ~1400 and 1500 cm⁻¹ are all associated with the coupled $\nu(\text{C}=\text{C})$ stretching vibration while the mode at ~1400 cm⁻¹, with the negative dν/dp value, is attributed to the mode with the largest $\nu(\text{C}=\text{C})$ component. No intensity changes between these modes were observed in any of the complexes, thus no changes in the extent of vibrational coupling with pressure can be established. The $\nu(\text{C}=\text{C})$ bands at ~1400 cm⁻¹ in the Raman spectra of Zeise's salt and the COD complex collapsed under high pressure. A similar observation has been

reported from a high-pressure vibrational study¹² on another π -bonded system with CN ligands. It was concluded that the increased occupation of the π^* -orbital with pressure induces a polarisation opposite to that of the bonding orbital with a resultant decrease in Raman intensity.

In the M-CO systems under pressure,¹⁻⁷ a large $d\nu/dp$ value for the $\nu(\text{M-CO})$ modes is paralleled by a simultaneous large decrease in the $\nu(\text{C=O})$ $d\nu/dp$ value. No such correlation was established between the pressure dependences of the $\nu(\text{Pt-C}_2\text{H}_4)$ and $\nu(\text{C=C})$ modes in any the complexes studied in this work. The $d\nu/dp$ values for the $\nu(\text{Pt-C}_2\text{H}_4)$ stretching modes are very high, 0.72 and 0.66 $\text{cm}^{-1} \text{kbar}^{-1}$, while those for the $\nu(\text{C=C})$ modes are relatively small, -0.08 $\text{cm}^{-1} \text{kbar}^{-1}$. In contrast, the COD complex has the largest negative $d\nu/dp$ value for $\nu(\text{C=C})$, -0.018 $\text{cm}^{-1} \text{kbar}^{-1}$, but the $\nu(\text{Pt-C}_2\text{H}_4)$ mode has a $d\nu/dp$ range of 0.31-0.45 $\text{cm}^{-1} \text{kbar}^{-1}$. This situation may be attributed to the differences in the ethylene orientation, the crystal lattices and the crystal packing forces. The perpendicular orientation of the ethylene bond in Zeise's salt is distorted to 85.90, this rotation being induced by the crystal packing forces.¹³ The frequency doublets in Zeise's dimer may be the result of a non-planar molecule or because of disymmetrical ethylene bonds. The COD complex has twisted ethylene bonds leading to C_2 symmetry. Thus, the observed negative pressure dependences of these ethylene bonds are the net result of π -backbonding and possibly further distortion of the ethylene bonds from their ideal perpendicular orientation due to increased crystal packing forces with increasing pressure, which would reduce the π -backbonding overlap. The K^+ ion in Zeise's salt [$\text{K}(\text{Pt}(\eta^2\text{-C}_2\text{H}_4)\text{Cl}_3)$] may also contribute. In other complexes, this cation is involved in strong cation-anion interactions, e.g., in $\text{K}_2[\text{PtCl}_4]$ ¹⁴ and in the high-pressure studies of $\text{A}[\text{MCl}_6]$ systems,¹⁵ where A = monovalent cation and M = Pt, Pd, Rh etc. This electrostatic interaction is absent in the other compounds investigated.

In all three compounds, the vibrational modes which shift the most upon coordination from those of free ethylene are the $\nu(\text{C=C})$, the coupled CH_2 scissoring and

the CH₂ twist modes.^{9,10} Under pressure, these modes exhibited the most diverse behaviour. The CH₂ twist mode in Zeise's salt and the dimer, at 736 and 721/725 cm⁻¹, respectively, both showed the largest $d\nu/dp$ values among the CH₂ deformation modes and the largest $d \ln\nu/dp$ values for modes appearing above the far-IR region. This particular mode is also coupled, the higher pressure dependence being a result of the magnitude of the actual CH₂ twist component. Therefore, the CH₂ twist in Pt(COD)Cl₂ was assigned to the 782 cm⁻¹ band on the basis of a similarly large $d \ln\nu/dp$ value of 0.44 cm⁻¹ kbar⁻¹.

The C-H stretching modes in Zeise's salt and the dimer display identical $d\nu/dp$ and $d \ln\nu/dp$ values, the symmetric and antisymmetric C-H stretching modes were further assigned from the observed $d\nu/dp$ values. The COD complex showed a wider range of C-H stretching $d\nu/dp$ values. The C₂ twist boat conformation induces a methylene H...H repulsion, and so the symmetric C-H stretching mode will be strongly restrained.¹⁸ There are two bands in this region at 3009 and 3023 cm⁻¹ with very small pressure dependences (0.25 and 0.30 cm⁻¹ kbar⁻¹, respectively). The less restrained antisymmetric C-H stretching modes are expected to have very large $d\nu/dp$ values and there are possibilities at 2911 and 2933 cm⁻¹ (1.35 and 1.32 cm⁻¹ kbar⁻¹, respectively).

REFERENCES

- (1) Huang, Y.; Butler, I. S.; Gilson, D. F. R. *Inorg. Chem.* **1990**, 30, 117.
- (2) Huang, Y.; Butler, I. S.; Gilson, D. F. R. *Inorg. Chem.* **1990**, 30, 1098.
- (3) Huang, Y.; Butler, I. S.; Gilson, D. F. R. *Spectrochim. Acta* **1991**, 47A, 909A
- (4) Adams, D. M.; Evejibiba, I. O. C. *J. Chem. Phys.* **1982**, 77, 4793.
- (5) Adams, D. M.; Evejibiba, I. O. C. *J. Chem. Phys.* **1983**, 78, 5408.
- (6) Adams, D. M.; Davey, L. M.; Hatton, P. D.; Shaw, A. C. *J. Mol. Struct.* **1982**, 79, 451.
- (7) Adams, D. M.; Hatton, P. D.; Sharn, A. C. *J. Chem. Soc., Chem. Commun.* **1981**, 226.
- (8) Baenziger, N. C.; Medud, R. C.; Doyle, J. R. *Acta Cryst.* **1964**, 18, 237.
- (9) Hirashi, J. *Spectrochim. Acta* **1967**, 25A, 749.
- (10) Grogan, M. J.; Makando, K. *J. Am. Chem. Soc.* **1966**, 88, 5453.
- (11) Mink, J.; Pápui, I.; Gái, M.; Goggin, P. L. *Pure Appl. Chem.* **1989**, 61, 973.
- (12) Wong, P. T. T. *J. Chem. Phys.* **1983**, 78, 4840.
- (13) Hartley, F. R. *Comp. Organ. Met. Chem.* **1982**, vol 6.
- (14) Goggin, P. L.; Mink, J. *J. Chem. Soc., Dalton Trans.* **1947**, 1479.
- (15) Adams, D. M.; Berg, R. W.; Williams, A. D. *J. Chem. Phys.* **1981**, 74, 2800.
- (16) Emer, O. *J. Am. Chem. Soc.* **1976**, 98, 3964.